PLoS one

Aerosol Chemistry over a High Altitude Station at Northeastern Himalayas, India

Abhijit Chatterjee[1], Anandamay Adak[1], Ajay K. Singh[2], Manoj K. Srivastava[3], Sanjay K. Ghosh[2,4], Suresh Tiwari[5], Panuganti C. S. Devara[6], Sibaji Raha[1,2,4]*

1 Environmental Sciences Section, Bose Institute, Kolkata, India, 2 Center for Astroparticle Physics and Space Science, Bose Institute, Kolkata and Darjeeling, India, 3 Department of Geophysics, Banaras Hindu University, Varanasi, India, 4 Department of Physics, Bose Institute, Kolkata, India, 5 Indian Institute of Tropical Meteorology, New Delhi, India, 6 Indian Institute of Tropical Meteorology, Pune, India

Abstract

Background: There is an urgent need for an improved understanding of the sources, distributions and properties of atmospheric aerosol in order to control the atmospheric pollution over northeastern Himalayas where rising anthropogenic interferences from rapid urbanization and development is becoming an increasing concern.

Methodology/Principal Findings: An extensive aerosol sampling program was conducted in Darjeeling (altitude ~2200 meter above sea level (masl), latitude 27°01′N and longitude 88°15′E), a high altitude station in northeastern Himalayas, during January–December 2005. Samples were collected using a respirable dust sampler and a fine dust sampler simultaneously. Ion chromatograph was used to analyze the water soluble ionic species of aerosol. The average concentrations of fine and coarse mode aerosol were found to be 29.5 ± 20.8 μg m^{-3} and 19.6 ± 11.1 μg m^{-3} respectively. Fine mode aerosol dominated during dry seasons and coarse mode aerosol dominated during monsoon. Nitrate existed as NH_4NO_3 in fine mode aerosol during winter and as $NaNO_3$ in coarse mode aerosol during monsoon. Gas phase photochemical oxidation of SO_2 during premonsoon and aqueous phase oxidation during winter and postmonsoon were the major pathways for the formation of SO_4^{2-} in the atmosphere. Long range transport of dust aerosol from arid regions of western India was observed during premonsoon. The acidity of fine mode aerosol was higher in dry seasons compared to monsoon whereas the coarse mode acidity was higher in monsoon compared to dry seasons. Biomass burning, vehicular emissions and dust particles were the major types of aerosol from local and continental regions whereas sea salt particles were the major types of aerosol from marine source regions.

Conclusions/Significance: The year-long data presented in this paper provide substantial improvements to the heretofore poor knowledge regarding aerosol chemistry over northeastern Himalayas, and should be useful to policy makers in making control strategies.

Introduction

Atmospheric aerosol is linked to visibility reduction, adverse health effects and heat balance of the Earth, directly by reflecting and absorbing solar radiation and indirectly by influencing the properties and cloud processes and, possibly, by changing the heterogeneous chemistry of reactive greenhouse gases [1]. The combined global radiative forcing due to increases in major greenhouse gases (CO_2, CH_4 and N_2O) is +2.3 Wm^{-2}. Anthropogenic contributions to aerosols (primarily sulphate, organic carbon, nitrate and dust) together produce a cooling effect, with a total direct radiative forcing of -0.5 Wm^{-2} and an indirect cloud albedo forcing of -0.7 Wm^{-2} [1]. Thus aerosols compensate by ~50% for the mean global radiative forcing due to greenhouse gases warming. The large range of uncertainty in estimating the aerosol forcing reflects the poor state of knowledge regarding the sources, distributions and properties of atmospheric aerosol.

Increasing pollutant emissions associated with the fast-growing economies of southeastern Asian countries have led to the progressive increase of aerosol concentrations above the natural background [2]. Satellite observations have shown that the light-absorbing aerosol hazes (which is about 3–5 mm thick) over India intensify over the Thar desert and the polluted Indo-Gangetic plain (IGP). The IGP has a sharp boundary to the north, where the Himalayas act as a barrier, extending thousands of miles southward and over the north Indian ocean [3,4]. Aerosol rich boundary layer air can be transported to higher altitudes by valley breezes on the Himalayan slopes [2].

The transport of optically-active aerosol to the higher Himalayas is a matter of concern, since most of the glaciers in the region have been retreating since 1850 [5] with increasing

melting rates, and are in danger of completely disappearing in the next decades [6]. If the retreat of the Himalayan glaciers continues unabated, it will exacerbate the water stress in northern India, especially during the dry season [7]. The rising anthropogenic interferences from rapid urbanization and development in the Himalayas affect both the landscape and the atmospheric environments and are the causes of increasing concern [8,9].

A short-term sampling program in the Nguzompa glacier basin near Mt. Everest [10], a two-week sampling project in Hidden Valley in the Himalayas of western Nepal [11], a year-long sampling of atmospheric aerosol at a remote Himalayan site and a rural Middle-Mountain site in Nepal [12], a study on the effect of mineral dust and carbonaceous species on the aerosol composition in Nepal Himalayas [13] and a study on the seasonal variation of total suspended particulates (TSP) in Manali, northwestern Himalayan range [14] are the major research studies carried out in the Nepal Himalayan and in other northwestern Himalayan sites. But as far as the northeastern Himalayas are concerned, the region still lacks systematic studies focused on chemical characterization of aerosols.

A strong seasonal variation in aerosol chemistry is expected in this northeastern Himalayan region. During premonsoon and summer months, due to enhanced convection, aerosols are lofted to elevated altitudes in the troposphere. Together with the westerly premonsoon winds, enhanced convection and the steep pressure gradient across the Himalayan-Gangetic region steer aerosols aloft. With the onset of rainy season (the Arabian Sea and Bay of Bengal branches of the South West summer monsoon), the heavy dust loading significantly diminishes due to aerosol washout from the atmosphere and enhances the loading of sea salt aerosols to a significant level. During winter and postmonsoon, northeasterly winds from the subcontinent bring anthropogenic aerosols over the Himalayan region. In addition to that, massive biomass burning during winter also plays a role in the loading of anthropogenic aerosols over northeastern Himalayas. These distinctly different seasonal behaviors of aerosol in northeastern Himalayas prompted us to make a year-long study on the formation and distribution of atmospheric aerosols over Darjeeling, a high altitude station in northeastern Himalayas.

In order to understand the seasonal nature of the predominant water soluble ionic species in fine (aerodynamic diameter less than 2.5 μm) and coarse mode (aerodynamic diameter more than 2.5 μm) aerosol a year-long aerosol sampling was done during January–December 2005. This study presents the possible formation mechanisms of secondary ionic species in different seasons, distribution of primary ionic species, long range transport of dust aerosol and the interaction between transported marine aerosol and locally generated anthropogenic aerosol. Finally, an attempt was made to find out the possible types of aerosols from different source regions.

The primary focus of this study was to determine the relative contribution of natural and anthropogenic components on the total aerosol loading and their distribution between fine and coarse mode aerosols at a high altitude hill station in northeastern Himalayas which could provide the scientific basis for controlling atmospheric pollution over this geo-politically and environmentally important region.

1. Site description

Darjeeling is one of the most popular tourist hill-stations in eastern India with a population of ~100,000. The overall areas of the Darjeeling district and Darjeeling Township are about 1200 and 11.44 squared kilometers, respectively. Darjeeling Township is located at an average altitude of ~2000 meter above sea level (masl) and surrounded by different types of topography of the lower-eastern-Himalayas. The southern region comprises the marshy low-lying area at an average height of ~100–300 masl. The apex is formed by the Phalut ridge (altitude of 3800 masl) at the border between Nepal and India. The eastern frontier lies along two rivers, locally called Tista and Rangeet.

The sampling site (shown in Figure 1) is located on the terrace of a three-storied building on our institute premises. This site (latitude: 27°01′N, longitude: 88°15′E with an altitude of 2194 masl) is at an altitude of about 200 m above the main township and is a remote area compared to the main township with a limited number of residential houses and forested areas dominated by juniper and varieties of pine in the immediate vicinity of the observatory. The closest street with significant road traffic is about 200 m away from the study site. The area, within a radius of ~10 km, is occupied by several major and minor tea processing units operated by furnace oil and coal and several tea gardens where several ammoniated fertilizers are used. Wood and biomass burning in the nearby villages, automobile exhaust (mainly tourist vehicles) throughout the year and the exhaust from the "Toy Train" (Darjeeling Himalayan Railway), which is enlisted as an UN (United Nations) world-heritage and still runs on coal as its fuel, are the major sources of air pollution at this hill station.

2. Prevailing meteorology

The monthly variations of surface meteorological parameters like temperature (°C), relative humidity (%), wind speed (m s^{-1}) along with total rainfall (mm) over the entire study period (Jan–Dec) are shown in Figure 2 and the surface wind directions presented seasonally in different seasons, namely, winter (Dec–Feb), premonsoon (Mar–May), monsoon (Jun–Sep) and postmonsoon (Oct–Nov) in Figure 3. The average temperature was found to be 15±4°C with minimum of 7°C during December and maximum of 20°C during June. In general, the relative humidity was high across the whole study period with an average of 81%. The dry season (Jan–May, Oct–Dec) remained moderately dry with an average relative humidity of 76% compared to the wet season with an average relative humidity of 91%. The total rainfall during the entire study period (Jan–Dec) was found to be 2220 mm, 80% of which was during southwest monsoon (1783 mm) with scanty or no rainfall during winter (20 mm) and premonsoon (304 mm). The surface wind pattern during winter was mainly easterly and northeasterly with average speed of 0.84 m s^{-1} and during monsoon it was mainly southwesterly with an average speed of 1.18 m s^{-1}. In order to know the wind pattern variations in different seasons, the monthly mean wind vectors (at 850 hPa level) for four different seasons; winter (Dec–Feb), premonsoon (Mar–May), monsoon (Jun–Sep) and postmonsoon (Oct–Nov) are shown in Figure 4, for the region covering equator to 40°N and 40–130°E. The NCEP/NCAR reanalysis data clearly show the contrasting wind patterns between winter and monsoon whereas premonsoon and postmonsoon represents the transition phase in the circulation patterns. Winter shows the weak northeasterly wind from the continental area covering densely populated cities including semi arid regions whereas monsoon shows strong southwesterly wind originating from Arabian Sea. These distinctly different wind fields impart extreme temporal variability in aerosol characteristics.

Methods

1. Collection of aerosol samples and determination of mass concentration

For the collection of total respirable suspended particulate matter (aerodynamic diameter less than 10 μm) from ambient air,

Figure 1. Map of the sampling station.
doi:10.1371/journal.pone.0011122.g001

a respirable dust sampler was used. The sampler (model APM 460BL) was manufactured by Envirotech Instrument Pvt Ltd, which pioneered the development of indigenous air monitoring instruments all over India. The sampler collected the samples with a flow rate of 1.4 m³ min⁻¹. The sampler was fitted with a cyclone, which was used for fractioning the dust into two fractions.

Total respirable particulate matter was collected on the filter paper (EPM 2000 filter paper from Whatman of 8″×10″ dimension) while particulate matter of aerodynamic diameter more than 10 μm was collected in a cup placed under the cyclone.

For collection of fine particulate matter or fine mode aerosol, a fine dust sampler was used from the same company (model APM
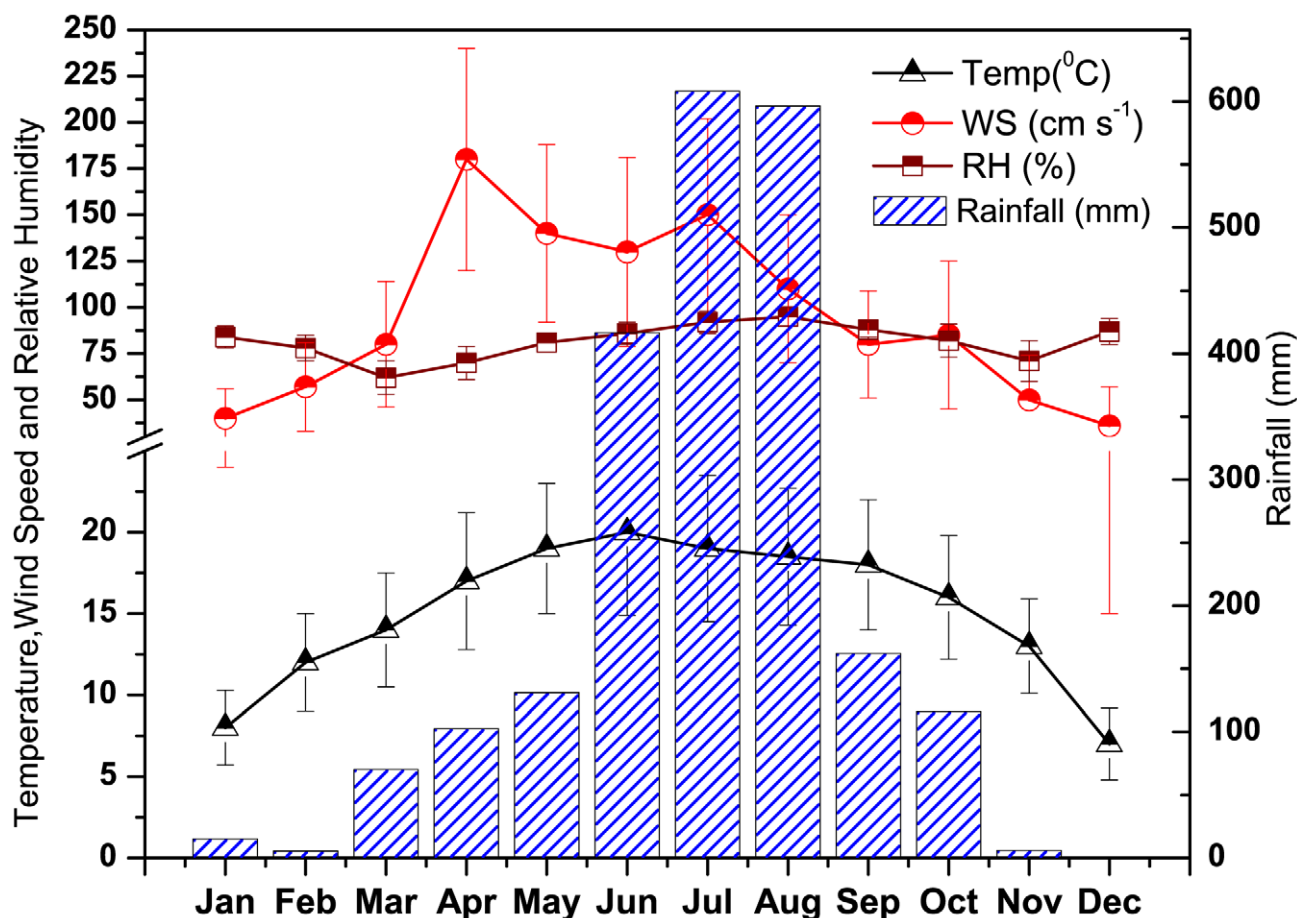
Figure 2. Seasonal variations of temperature (Temp), wind speed (WS), relative humidity (RH) and rainfall over Darjeeling.
doi:10.1371/journal.pone.0011122.g002

550). The flow rate was 1 $m^3 hr^{-1}$. After entering the air particles through the inlet of the sampler the coarse particulate matter (aerodynamic diameter more than 2.5 µm) was removed using a GF/A (Glass Fiber) filter paper of 37 mm diameter immersed in silicone oil, used as an impaction surface. The impaction surface was placed above the main aerosol collection filter. The fine particles were collected on a PTFE filter paper of 47 mm diameter.

On average, an aerosol sample (both for fine and total respirable particulate matter) was collected on every 3rd day during dry seasons (Jan–May, Oct–Dec) and every 4th day during monsoon (Jun–Sep). Thus a total of 111 samples were collected (81 during dry season and 30 during monsoon). Although collection of samples on daily basis would be better in carrying out this kind of aerosol study, collection of samples of more than 111 were beyond our scope. Each sampling was started at 0900 hrs (local time) and run for ~24 hrs. Both the samplers were placed on the terrace of a three-storied building (~15 m above ground level) on our institute premises.

The mass concentration of aerosol was determined by the gravimetric measurement. The filters were placed in desiccators for ~24 hrs before and after the sampling to remove the absorbed water and weighed in a controlled environment chamber after taking the filters out of the desiccators before and after the sampling using a semi-micro balance (Sartorius, Model ME 235 P). The aerosol mass (µg) was determined by the differences between initial and final weight of the filter and the concentration

(µg m^{-3}) was determined dividing the aerosol mass by total volume of air (m^3).

2. Meteorological parameters

The meteorological parameters were recorded with the help of an automatic weather station of Lawrence & Mayo (Model: AWS-PC) and all the data were run by LYNX-software of version V0007. The weather station was run continuously and the data were recorded at the interval of half an hour throughout the year covering all the sampling events. The weather station was equipped with a tower and all the sensors of wind speed and its direction, relative humidity (RH) and temperature were fitted with that tower at a height of 15 m from the ground level. The rainfall data was obtained from Indian Meteorological Department, India.

3. Chemical analysis

For the analysis of water soluble ions, chromatographic separation method was used [15]. One-half of the filters were soaked in 20 ml Milli-Q water (18.2 MΩ resistivity) for ~30 min. and ultrasonicated for 20 min. The solutions were made up to known volume (100 ml) using Milli-Q water. The solutions were then kept in polypropelene bottles and kept at ~4°C until analysis. Prior to their use, the bottles were cleaned repeatedly using distilled water and soaked for ~72 hrs. The major ions, namely anions (Cl^-, NO_3^- and SO_4^{2-}) and cations (Na^+, NH_4^+, K^+, Ca^{2+} and Mg^{2+}) were quantitatively determined by Ion Chromatograph (DIONEX-2000, USA) using analytical column IonPac ® AS15
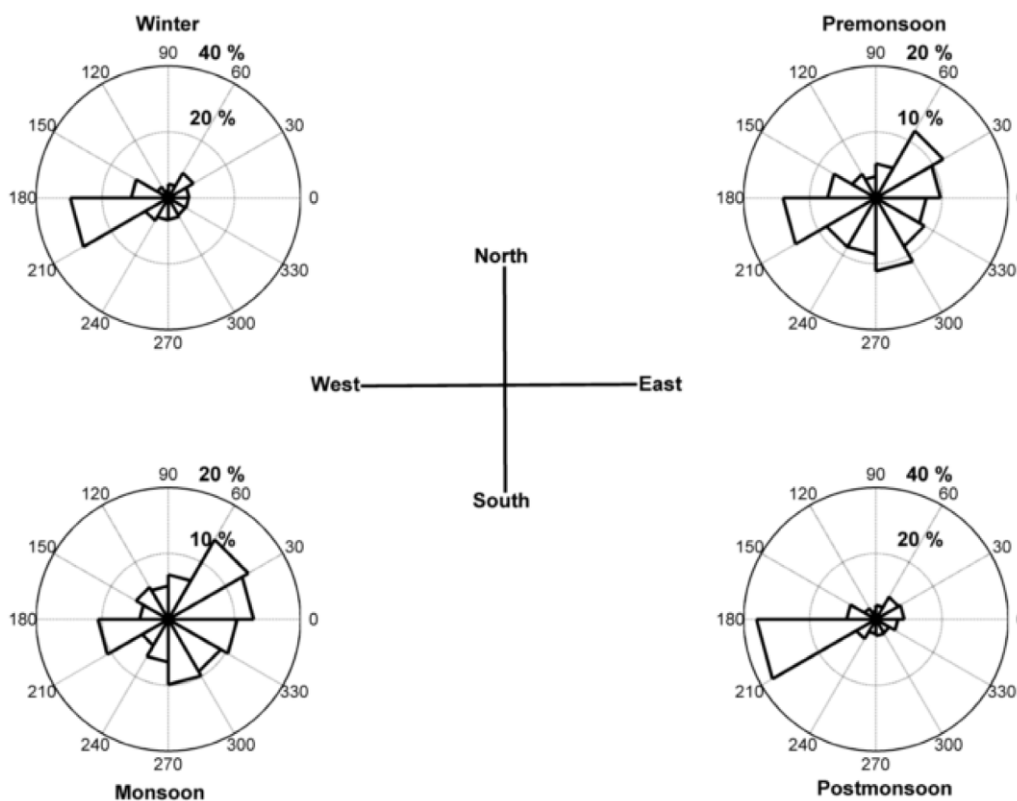
Figure 3. Rose diagram of surface wind speed and direction over the entire study period in Darjeeling.
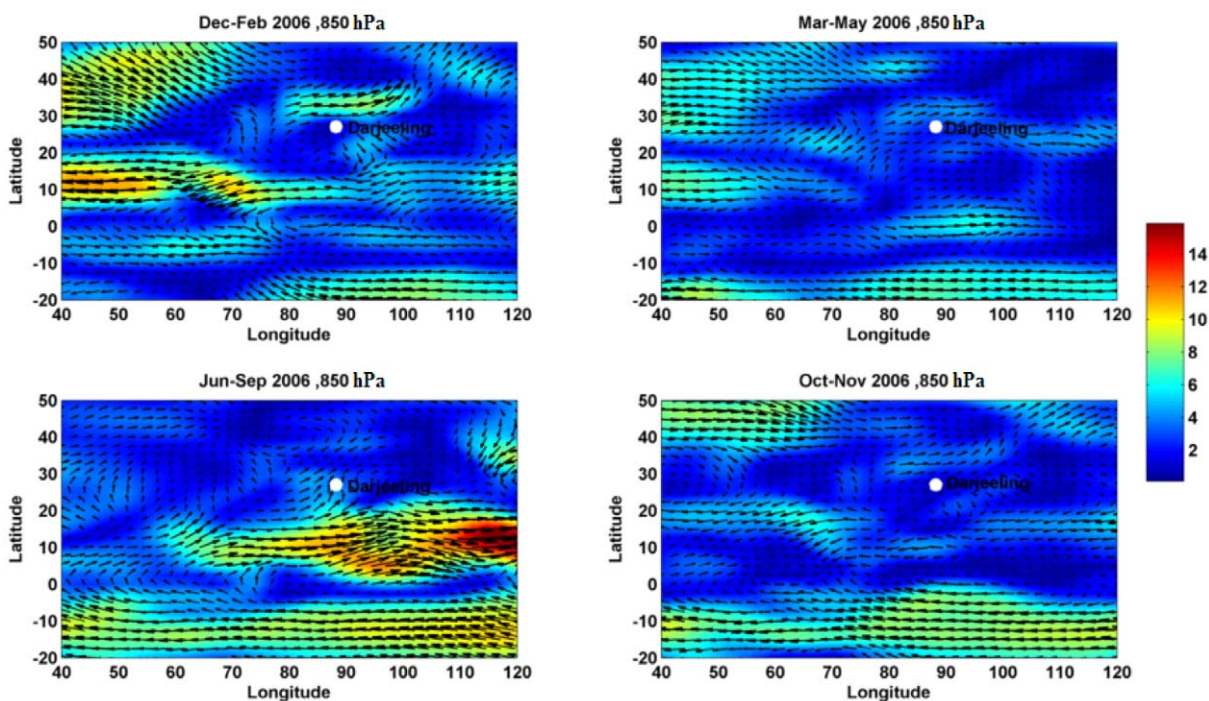doi:10.1371/journal.pone.0011122.g003

Figure 4. Mean wind at 850 hPa level obtained from NCEP/NCAR reanalysis during different seasons over Darjeeling.
doi:10.1371/journal.pone.0011122.g004

with micro-membrane suppressor ASRS ultra II 2mm, 38 mM. KOH as eluent and triple distilled water as regenerator for anions. Similarly, the IonPac ® CS17 column with micro-membrane suppressor CSRS ultra II 2mm, 6 mM methansulfonic acid as eluent and triple distilled water as regenerator were used for cations. For calibration purpose, the standards were procured from Dionex for cations and anions. Detection limits of the ionic species, concentrations corresponding to three times the standard deviation of five replicate blank level measurements for Na^+, K^+, Ca^{2+}, Mg^{2+}, NH_4^+, Cl^-, NO_3^- and SO_4^{2-} were 0.009, 0.0013, 0.003, 0.0015, 0.0024, 0.009, 0.005 and 0.008 $\mu g\,m^{-3}$ respectively. The precision estimated from the standard deviation of repeat measurements of standard and samples was 2% for Na^+, K^+ and Ca^{2+}; 3% for Mg^{2+}; 5% for NH_4^+; 2% for Cl^-, SO_4^{2-} and 4% for NO_3^-. Trace gas SO_2 was measured using an on-line SO_2 analyzer (Horiba, APSA-360A) throughout all the sampling events at five minute interval.

Results and Discussion

1. Seasonal variation of particulate matter

The average concentration of fine mode aerosol in Darjeeling was found to be 29.5±20.8 $\mu g\,m^{-3}$ varying between 3.6 $\mu g\,m^{-3}$ and 61 $\mu g\,m^{-3}$, whereas coarse mode aerosol ranged between 5.4 $\mu g\,m^{-3}$ and 32 $\mu g\,m^{-3}$ with an average of 19.6± 11.1 $\mu g\,m^{-3}$. The large variation in concentrations of both fine

and coarse mode aerosol (Figure 5) during the entire study period could be due to the thermodynamic conditions in the planetary boundary layer (PBL), which either favor or adversely affect pollutants dispersion. Ambient weather conditions, such as air temperature, relative humidity and short wave radiation, could also influence the chemical reactions leading to secondary aerosol formation. Stable atmospheric conditions with a low mixing layer height may result in significantly enhanced particulate concentrations [16]. Aerosol shows higher concentrations during winter months and minimum concentrations during monsoon. In winter, very frequent and persistent thermal inversion and fog situations at ground level caused a considerable amount of aerosol to accumulate in the lower layers of the atmosphere [17]. Aerosol concentrations during winter were largely affected due to massive biomass burning over Darjeeling. The higher emission of K^+, SO_4^{2-} and carbonaceous species (not analyzed for the present study) could enhance the aerosol loading in the atmosphere during winter. The sharp fall in fine mode aerosol concentrations and high precipitation amount (1783 mm) during monsoon indicates the wash out effect of aerosol and its components. On the other hand, the coarse mode aerosol did not show a sharp decrease in concentrations during monsoon due to the contribution of sea salt aerosol (Na^+, Cl^-, Mg^{2+}). Non-sea-sulphate and nitrate were also found to enhance the coarse mode aerosol concentrations during monsoon (discussed later in detail). The ratios of fine to coarse mode aerosol concentrations were found to widely vary between
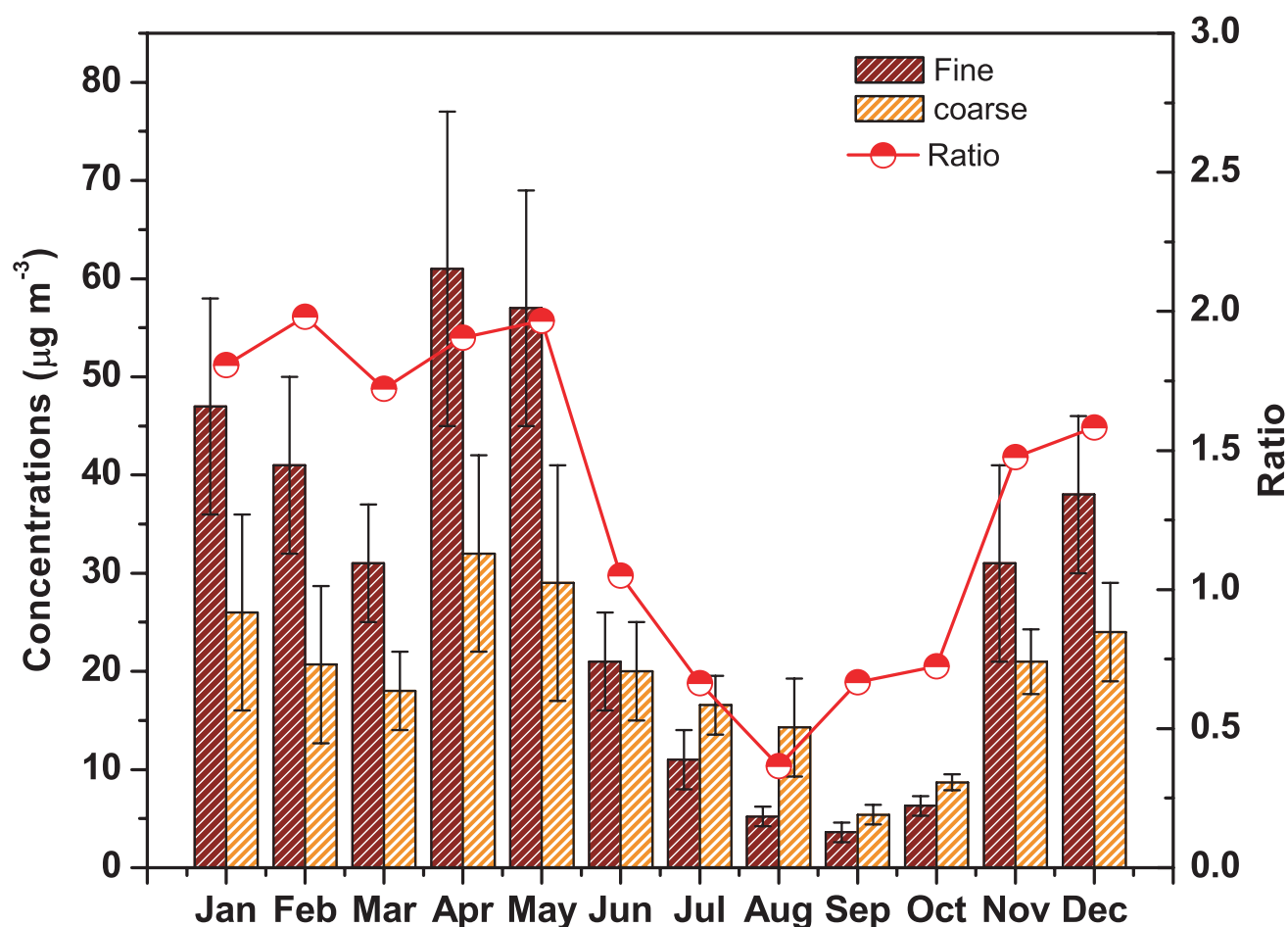

Figure 5. Seasonal variations of aerosol over Darjeeling.
doi:10.1371/journal.pone.0011122.g005

Table 1. Comparison of this study with other high altitude stations in India and Nepal.

	Darjeeling Northeastern Himalayas, India		Nagarkot, Nepal Himalayas	Langtang, Nepal Himalayas	Phortse, Nepal Himalayas	Jiri, Nepal Himalayas	Manora Peak, India	Khumbu valley, Nepal	Mt Abu, Western India
References	This study		[13]	[13]	[12]	[12]	[42]	[7]	[19]
Altitude(masl)	2194		2150	3920	4100	1900	1950	5079	1680
Aerosol type	Fine	Coarse	Fine	Fine	PM_{10}	PM_{10}	TSP	PM_{10}	TSP
Samples	111	111	NA	NA	17	13	NA	13	25
Na^+	0.66±0.43	2.20±2.00	0.20±0.16	0.12±0.18	0.03	0.08	NA	NA	0.28
NH_4^+	0.88±0.76	0.05±0.04	1.50±1.00	0.54±0.56	0.28	0.35	0.52	0.14	0.37
K^+	1.20±0.80	0.31±0.21	0.62±0.58	0.20±0.26	0.15	0.25	0.23	0.02	0.20
nsK^+	1.15±0.82	0.23±0.20	0.61	NA	NA	NA	NA	NA	NA
Ca^{2+}	0.13±0.01	0.40±0.20	0.31±0.29	0.66±0.89	0.12	0.56	0.75	0.10	1.70
$nsCa^{2+}$	0.11±0.10	0.38±0.21	NA	NA	NA	NA	NA	NA	NA
Mg^{2+}	0.12±0.06	0.31±0.17	0.04±0.03	0.05±0.05	0.03	0.08	NA	NA	0.09
$nsMg^{2+}$	0.04±0.03	0.14±0.18	NA	NA	NA	NA	NA	NA	NA
Cl^-	1.21±1.00	2.35±1.50	0.05±0.05	0.06±0.10	0.01	0.01	NA	NA	0.31
$nsCl^-$	0.44±0.41	−0.18±1.10	NA	NA	NA	NA	NA	NA	NA
NO^{3-}	3.31±2.30	0.95±0.20	1.20±1.80	0.78±0.10	0.70	0.48	0.50	0.08	0.74
SO_4^{2-}	3.80±2.90	2.50±2.10	3.80±1.00	1.41±1.30	0.98	0.41	2.60	0.22	2.71
$nsSO_4^{2-}$	3.64±2.80	1.92±1.84	NA	NA	NA	NA	NA	NA	NA

NA: Not Available; Concentrations of ionic species are given in µg m^{-3}.
doi:10.1371/journal.pone.0011122.t001

0.36 (during August) and 4.4 (during January) with an average of 1.4±1.1. On an average, the average ratio of 1.72 was observed during dry seasons and 0.76 during monsoon. Thus, fine mode aerosol dominated over coarse mode aerosol during dry seasons whereas coarse mode aerosol dominated over fine mode aerosol during monsoon. A peak was observed in aerosol concentrations both in fine and coarse mode during two premonsoon months, April and May. This could be attributed to the long range transport of dust aerosol from arid regions of western India and even from Arabian deserts (discussed later in detail) during

Table 2. Comparison of this study with other urban sites in India.

	Darjeeling, Northeastern Himalayas, India		Mumbai, India	Pune, India	Agra, India	Ahmedabad, India
References	This study		[43]	[9]	[44]	[19]
Altitude(masl)	2194					
Aerosol type	Fine	Coarse	PM_{10}	PM_{10}	TSP	TSP
Samples	111	111	NA	NA	NA	25
Na^+	0.66±0.43	2.20±2.00	2.20	0.48	2.97	0.81
NH_4^+	0.88±0.76	0.05±0.04	NA	2.14	6.52	0.48
K^+	1.20±0.80	0.31±0.20	8.90	0.43	2.50	0.76
nsK^+	1.15±0.82	0.23±0.20	NA	NA	NA	0.73
Ca^{2+}	0.13±0.01	0.40±0.20	6.20	2.50	3.02	2.96
$nsCa^{2+}$	0.11±0.10	0.38±0.20	NA	NA	NA	2.93
Mg^{2+}	0.12±0.06	0.31±0.17	2.20	0.23	1.24	0.25
$nsMg^{2+}$	0.04±0.03	0.14±0.18	NA	NA	NA	0.15
Cl^-	1.21±1.00	2.35±1.50	2.60	1.80	6.78	0.99
$nsCl^-$	0.44±0.41	−0.18±1.10	NA	NA	NA	NA
NO^{3-}	3.31±2.30	0.95±0.20	6.00	2.91	8.37	2.07
SO_4^{2-}	3.80±2.90	2.50±2.10	6.20	2.98	14.7	4.57
$nsSO_4^{2-}$	3.64±2.80	1.92±1.84	NA	NA	NA	4.36

NA: Not available; Concentrations of ionic species are given in µg m^{-3}.
doi:10.1371/journal.pone.0011122.t002

Table 3. Inter-ionic correlations in fine and coarse mode aerosols over Darjeeling during dry seasons (n = 81).

	Na^+	NH_4^+	K^+	nsK^+	Ca^{2+}	$nsCa^{2+}$	Mg^{2+}	$nsMg^{2+}$	Cl^-	NO_3^-	SO_4^{2-}	$nsSO_4^{2-}$
Na^+		F=0.35 C=0.14	F=0.24 C=0.21	F=0.16 C=0.13	F=0.26 C=0.23	F=0.18 C=0.39	F=0.13 C=0.19	F=0.11 C=0.29	F=0.38 C=0.44	F=0.17 C=0.11	F=0.19 C=0.37	F=0.14 C=0.26
NH_4^+			F=0.12 C=0.16	F=0.19 C=0.31	F=0.11 C=0.10	F=0.17 C=0.21	F=0.22 C=0.20	F=0.19 C=0.14	F=0.23 C=0.10	F=0.74 C=0.51	F=0.44 C=0.42	F=0.65 C=0.44
K^+					F=0.18 C=0.38	F=0.21 C=0.34	F=0.16 C=0.18	F=0.14 C=0.34	F=0.26 C=0.37	F=0.11 C=0.15	F=0.19 C=0.27	F=0.29 C=0.27
nsK^+					F=0.29 C=0.31	F=0.31 C=0.21	F=0.11 C=0.20	F=0.13 C=0.42	F=0.82 C=0.57	F=0.19 C=0.27	F=0.39 C=0.17	F=0.78 C=0.37
Ca^{+2}							F=0.55 C=0.62	F=0.48 C=0.42	F=0.19 C=0.22	F=0.19 C=0.27	F=0.22 C=0.31	F=0.11 C=0.25
$nsCa^{2+}$							F=0.39 C=0.54	F=0.64 C=0.74	F=0.10 C=0.17	F=0.10 C=0.22	F=0.31 C=0.37	F=0.20 C=0.12
Mg^{+2}								F=0.23 C=0.31	F=0.10 C=0.17	F=0.32 C=0.31	F=0.25 C=0.27	
$nsMg^{2+}$									F=0.30 C=0.12	F=0.16 C=0.17	F=0.15 C=0.17	F=0.11 C=0.26
Cl^-										F=0.19 C=0.15	F=0.29 C=0.48	F=0.78 C=0.37
NO_3^-											F=0.58 C=0.33	F=0.55 C=0.41
SO_4^{-2}												
$nsSO_4^{2-}$												

premonsoon. According to the elevated heat pump (EHP) mechanism proposed in [18] the dust aerosols mixed with carbonaceous aerosols primarily from Indo-Gangetic Plain (IGP) reaches the foothills of the Himalayas and are vertically advected to elevated altitudes. This causes significant loading of aerosol over the Himalayan region during premonsoon. The carbonaceous aerosol components and the trace elements (mainly the mineral dust component) data, though not analyzed for the present study, would provide better information on the high aerosol loading over Darjeeling during premonsoon.

2. Water-soluble ionic species in aerosol

2.1. Comparison with other studies over Himalayan region and Indian subcontinent. Water-soluble inorganic ions (Na^+, NH_4^+, K^+, Ca^{2+}, Mg^{2+}, Cl^-, NO_3^-, SO_4^{2-}) in fine and coarse mode aerosol over Darjeeling have been compared with the data reported in other high altitude stations in India and Nepal and other sites in Indian subcontinent.

For comparison with other high altitude stations, seven such stations (five in Nepal and two in India) have been chosen (Table 1). It is observed that the concentrations of sodium and chloride are several times higher than all the other hill stations indicating the strong influence of sea salt aerosol over Darjeeling. The most interesting feature is that in addition to the strong influence of sea salt aerosol, massive coal and biomass burning (domestic, industrial and from Darjeeling Himalayan Railways) throughout the year enhanced the concentration of non-sea-Cl^- in fine mode aerosol over Darjeeling. The concentrations of ammonium, nitrate and sulphate, the secondary anthropogenic ionic species in aerosol over Darjeeling, are 3–15 times higher than all the other hill stations except Nagarkot. The concentration of NH_4^+ in Nagarkot is higher than all the hill stations due to the close proximity of the sampling station to agricultural land and animal husbandry. The higher vehicular activities due to the high influx of tourists in Darjeeling could be the reason behind the higher loading of nitrate. Strong influence of massive biomass burning in Darjeeling was observed in the very high concentrations of non-sea-SO_4^{2-} and non-sea-K^+. When we compared the Ca^{2+} concentration, we noticed that our data do not differ significantly from the other high altitude stations. The concentration of Ca^{2+} varied between 0.12 $\mu g\ m^{-3}$ and 0.75 $\mu g\ m^{-3}$ in various stations in Himalayas (including Darjeeling), located between 1900 (Jiri, Nepal) and 5079 (NCO-P, Nepal) masl. Therefore, Ca^{2+} seems to be more homogeneously distributed vertically in Himalayan regions compared to other ionic species. The loading of dust aerosol enriched with Ca^{2+} in Himalayan region is mostly due to the long-range transport of dust aerosol originated in the western part of India (discussed later). However, the Ca^{2+} concentration over Mt. Abu in western India shows the highest concentration which is due to the widespread marble queries and stone-crushing mills in plain lands along the Aravali range in western India [19]. Mg^{2+} in the present study shows the highest concentration compared to the other sites. But if we look at the fine mode Mg^{2+} only, we find that our data do not significantly differ from the other sites (varying between 0.03 and 0.12 $\mu g\ m^{-3}$) indicating homogeneous vertical distribution of Mg^{2+}, like Ca^{2+}, in Himalayan regions.

The comparison of the data of aerosol ionic species of the present study with four urban sites (including a mega city, Mumbai) in India is shown in Table 2. It is observed from the table that, Na^+ and Cl^- are higher in concentrations than Pune and Ahmedabad and comparable to Agra, but the most interesting feature is that the concentrations of Na^+ and Cl^- in Darjeeling are found to be higher than at Mumbai, a coastal city in western India. At this stage, we could not find a fool-proof explanation for this most interesting observation; further, long-term study is required to understand this phenomenon. NH_4^+ and NO_3^- in Darjeeling are found to show lower concentrations than at Mumbai, Pune or Agra. K^+ and SO_4^{2-} show higher concentrations in Darjeeling
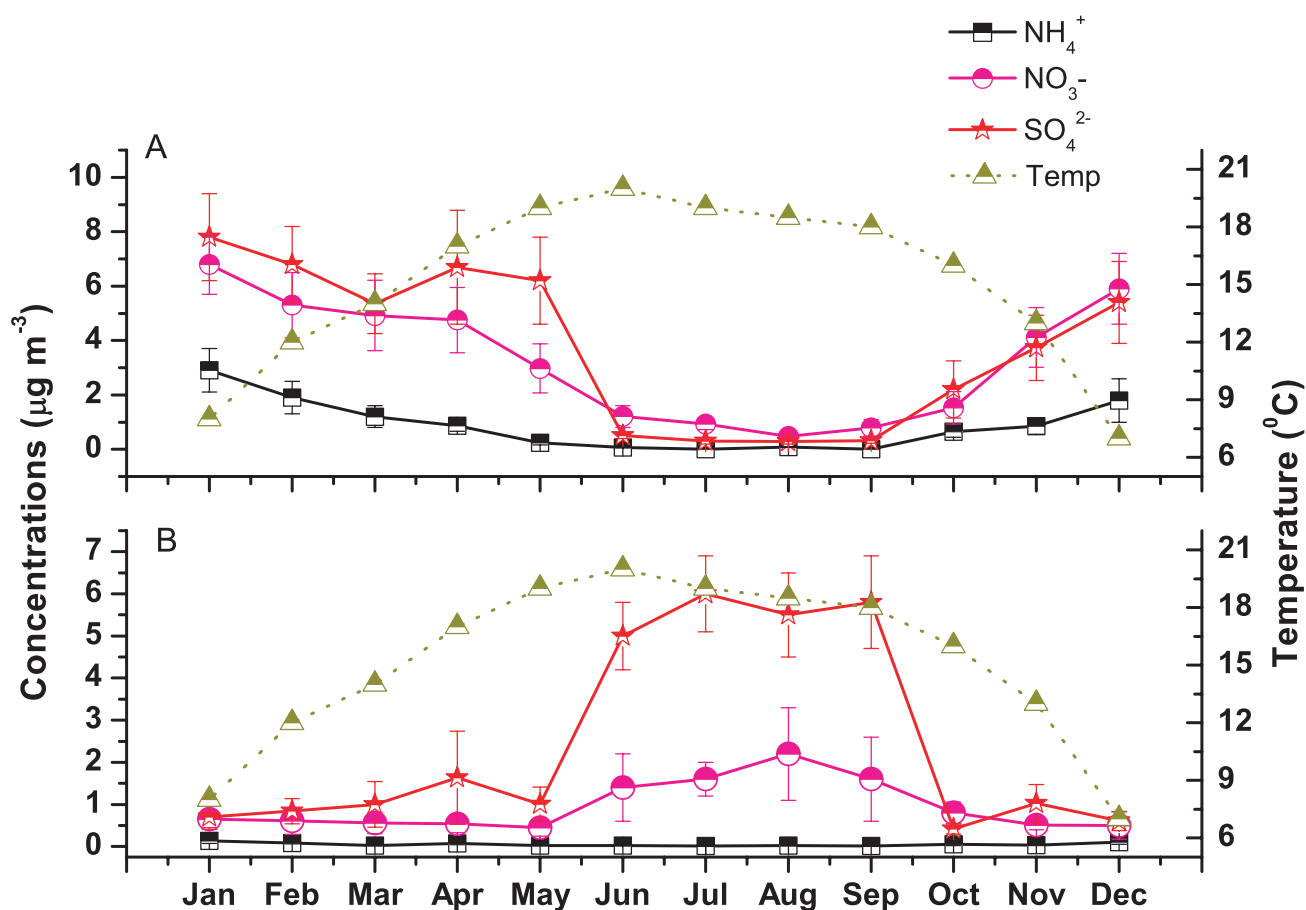
Figure 6. Seasonal variations of secondary ionic species and temperature over Darjeeling.
doi:10.1371/journal.pone.0011122.g006

than at Pune and Ahmedabad whereas we observed a similarity in SO_4^{2-} concentrations between Darjeeling and Mumbai. The concentrations of Ca^{2+} over all the urban sites are found to be higher than that over Darjeeling. The very high Ca^{2+} concentration over Ahmedabad is due to its close proximity to Thar deserts. On the other hand, the concentration of Mg^{2+} in Darjeeling is found to be higher than Pune and Ahmedabad and lower than Mumbai and Agra.

Conclusively, we observed that Darjeeling in northeastern Himalayas is strongly influenced by the sea salt and anthropogenic aerosol which are higher than all the high altitude stations in Indian and Nepal Himalayan region and even higher than most of the urban regions in India, compared with the present study. On the other hand, dust aerosol is found to be homogeneously distributed vertically between all the Himalayan regions but is significantly lower than urban regions in India.

2.2. Secondary ionic species in fine and coarse mode aerosol. NH_4^+, NO_3^- and SO_4^{2-}, the secondary components of aerosol, constituted $67.8 \pm 5.9\%$ fine mode and $36.4 \pm 10.07\%$ coarse mode aerosol in Darjeeling. The average concentrations of NH_4^+, NO_3^- and SO_4^{2-} in fine and coarse mode aerosol were 0.88 ± 0.76 μg m^{-3}, 3.31 ± 2.25 μg m^{-3}, 3.8 ± 2.9 μg m^{-3} and 0.05 ± 0.04 μg m^{-3}, 0.95 ± 0.17 μgm^{-3}, 2.5 ± 2.1 μg m^{-3}, respectively.

NH_4^+ and NO_3^- in fine mode aerosol showed higher enrichment (~ 15 times and 4 times, respectively) compared to coarse mode aerosol. This is due to the fact that gas to particle conversion of gas phase HNO_3 and NH_3 to particulate NO_3^- and

NH_4^+ are more feasible in nucleation (<0.1μm) and accumulation mode (>0.1 μm <2.5 μm) particles [20]. NH_4^+ and NO_3^- show good correlation (with correlation coefficient, $R^2 = 0.74$ and number of samples, $n = 81$) (Table 3) between each other in fine mode aerosol during dry seasons. Figure 6 shows the month wise variations in secondary species concentrations along with ambient temperature both in fine and coarse mode aerosol. The variation of fine mode NH_4^+ and NO_3^- are similar in nature showing a gradual decrease in concentrations from the month of January with a minimum during monsoon and a gradual increase till December which is exactly opposite in nature with respect to the ambient temperature variations. The higher NH_4^+ concentrations during winter is under the influence of NE wind transporting the large-scale pollutants whereas the lower concentration of NH_4^+ in monsoon suggests the dominant occurrence of NH_4^+ in gas phase [19].

The higher concentration of particulate ammonium and nitrate in winter was due to the shifting from the gas phase of nitric acid to the particulate phase of nitrate at lower temperature. The formation of particulate NH_4NO_3 is given by the following equilibrium

$$NH_3(g) + HNO_3(g) \leftrightarrow NH_4NO_3(s)$$
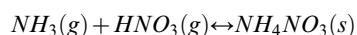
The equilibrium shifts towards the left side at higher temperature as NH_4NO_3 volatilizes when temperature increases [21]. We observed a gradual decrease in fine mode ammonium and nitrate
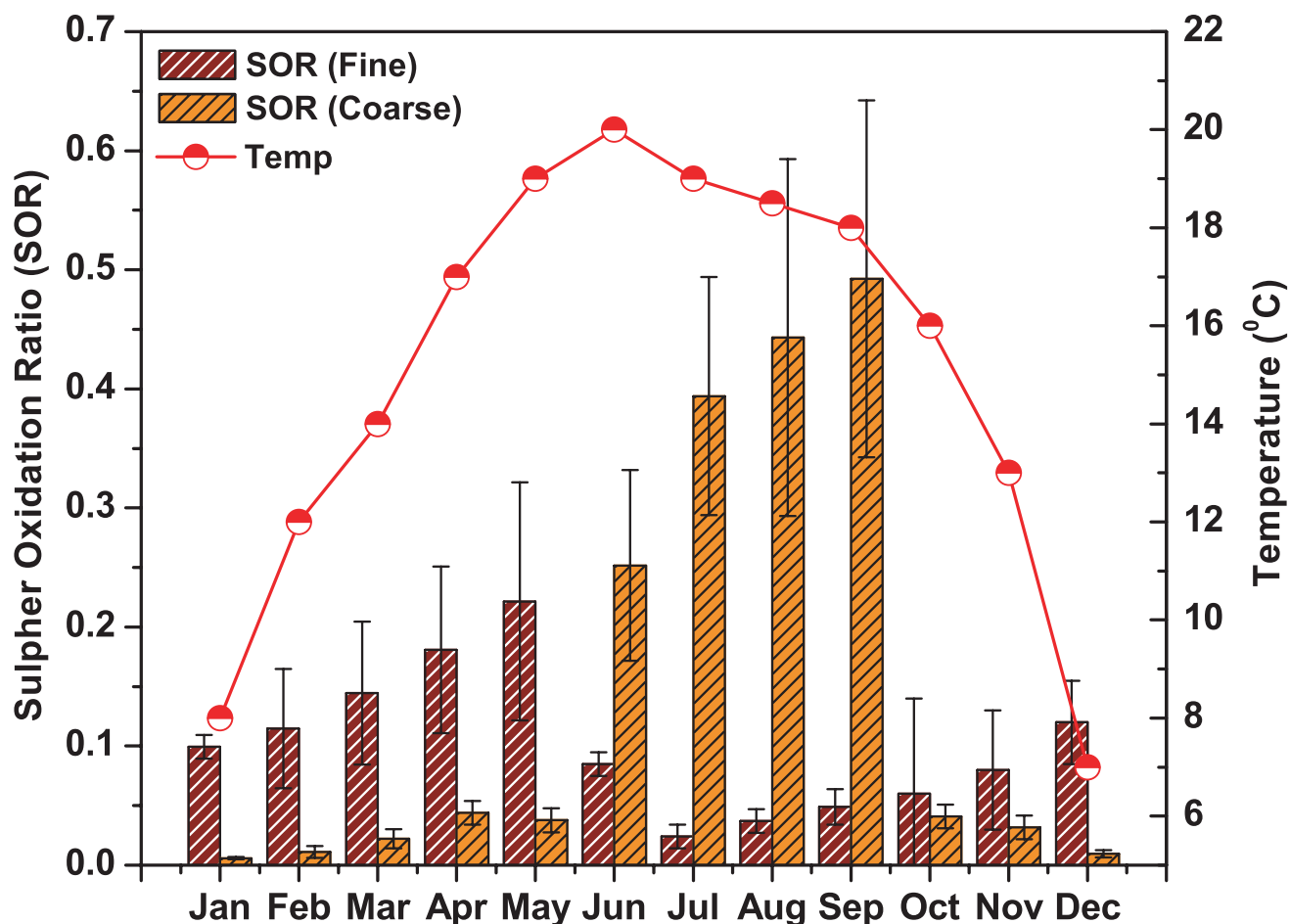
Figure 7. Different mechanisms of sulphate production over Darjeeling in different seasons.
doi:10.1371/journal.pone.0011122.g007

concentrations from January as temperature increases. Also, when there is significant production of sulphate by reaction between OH radical and SO_2, then sulphate acts as a sink for ammonia. Once ammonia becomes ammonium bisulphate or ammonium sulphate, ammonium becomes unavailable for nitrate [22]. We observed the high sulphate production in fine mode aerosol through SO_2 oxidation by OH radical (discussed in section 4.2) during premonsoon. While fine mode nitrate shows minimum concentrations during monsoon due to the wash out effect or below cloud scavenging, the coarse mode NO_3^- shows higher concentrations during monsoon compared to the dry seasons. The presence of sea salt aerosol may favor the formation of coarse mode NO_3^- as $NaNO_3$ by up taking of nitrogen oxides and HNO_3 on the surface of sea salt aerosol [23]. Many investigators have observed that the depletion of Cl^- from sea salt aerosol and the simultaneous occurrence is particularly pronounced in coarse particle, typical of sea salt aerosol [23]. The role of nitrate in chloride depletion from sea salt aerosol has been discussed in detail in section 4.2.

The sulfur oxidation ratio defined as $SOR = \dfrac{non-sea-SO_4^{2-}}{(non-sea-SO_4^{2-}+SO_2)}$ was used as an indicator of the secondary transformation process and the formation route and source of sulphate in the atmosphere. Figure 7 shows the month wise variation of SOR with temperature for both fine and coarse mode aerosol. The ratio varied between 0.03 and 0.22 with an average of 0.11±0.07 in fine mode aerosol and between 0.006 and

0.49 with an average of 0.15±0.14 in coarse mode aerosol. SORs in fine mode aerosol were found to increase gradually with the temperature and higher values were observed during premonsoon. When the ratio value is greater than 0.10, then there would be the occurrence of the photochemical oxidation of SO_2 in the atmosphere [24]. This indicates that gas phase photochemical oxidation of SO_2 followed by the condensation and absorption into the particle phase was the most important pathway for the production of fine mode SO_4^{2-} in the atmosphere during premonsoon (SOR>0.1). The gas phase oxidation of SO_2 to SO_4^{2-} by OH radical is a strong function of temperature [25]. The comparatively lower SOR during the winter months for both the fine and coarse mode aerosols indicate some aqueous phase transformation processes such as metal catalyzed oxidation of SO_2, aqueous phase H_2O_2/O_3 oxidation of SO_2 etc. Similar observation was also made in [26]. On the other hand, the very high SOR in coarse mode aerosol during monsoon could be due to the absorption of SO_2 by the soil dust particles at higher relative humidity during monsoon to form coarse mode sulphate of crustal origin [19,27]. Table 4 shows strong correlations (with correlation coefficient, $R^2 = 0.68$ and number of samples, n = 30) non-sea-SO_4^{2-} and non-sea-Ca^{2+} and between non-sea-SO_4^{2-} and non-sea-Mg^{2+} ($R^2 = 0.68$, n = 30) in coarse mode aerosol during monsoon.

2.3. Primary ionic species in fine and coarse mode aerosol. Na^+ and Cl^- constituted 16.6±5.46% fine mode and

Table 4. Inter-ionic correlations in fine and coarse mode aerosols over Darjeeling during monsoon (n = 30).

	Na$^+$	NH$_4^+$	K$^+$	nsK$^+$	Ca^{2+}	nsCa^{2+}	Mg^{2+}	nsMg^{2+}	Cl$^-$	NO$_3^-$	SO$_4^{2-}$	nsSO$_4^{2-}$
Na$^+$		F=0.15 C=0.14	F=0.14 C=0.11	F=0.17 C=0.22	F=0.10 C=0.11	F=0.19 C=0.23	F=0.15 C=0.23	F=0.17 C=0.31	F=0.68 C=0.89	F=0.12 C=0.83	F=0.29 C=0.39	F=0.78 C=0.21
NH$_4^+$			F=0.16 C=0.19	F=0.21 C=0.41	F=0.23 C=0.31	F=0.11 C=0.22	F=0.09 C=0.13	F=0.08 C=0.03	F=0.15 C=0.10	F=0.14 C=0.31	F=0.11 C=0.12	F=0.10 C=0.14
K$^+$					F=0.11 C=0.18	F=0.16 C=0.11	F=0.05 C=0.11	F=0.03 C=0.02	F=0.13 C=0.09	F=0.11 C=0.19	F=0.23 C=0.16	F=0.09 C=0.07
nsK$^+$					F=0.39 C=0.13	F=0.10 C=0.21	F=0.11 C=0.08	F=0.10 C=0.06	F=0.08 C=0.02	F=0.19 C=0.31	F=0.29 C=0.11	F=0.33 C=0.41
Ca^{+2}							F=0.20 C=0.32	F=0.11 C=0.12	F=0.09 C=0.06	F=0.10 C=0.25	F=0.21 C=0.30	F=0.14 C=0.15
nsCa^{2+}							F=0.19 C=0.04	F=0.16 C=0.13	F=0.15 C=0.12	F=0.13 C=0.21	F=0.08 C=0.06	F=0.13 C=0.72
Mg^{+2}								F=0.33 C=0.68	F=0.13 C=0.03	F=0.12 C=0.06	F=0.07 C=0.06	
nsMg^{2+}									F=0.11 C=0.03	F=0.16 C=0.02	F=0.04 C=0.10	F=0.09 C=0.68
Cl$^-$										F=0.21 C=0.15	F=0.31 C=0.58	F=0.09 C=0.07
NO$_3^-$											F=0.15 C=0.15	F=0.16 C=0.13
SO$_4^{-2}$												
nsSO$_4^{2-}$												

46.2±11.14% coarse mode aerosol. The average concentrations of Na$^+$ and Cl$^-$ in fine and coarse mode aerosol were found to be 0.66±0.43 µg m^{-3}, 1.21±1.00 µg m^{-3} and 2.16±2.01 µg m^{-3}, 2.35±1.5 µg m^{-3} respectively. The seasonal distribution of Na$^+$ and Cl$^-$ in coarse mode aerosol is similar in nature with the higher concentrations during monsoon. But the concentration of fine mode Cl$^-$ was found to be higher during the winter months and minimum during monsoon (Figure 8).

During monsoon, the correlation between coarse mode Na$^+$ and Cl$^-$ was found to be very strong (R^2 = 0.89, n = 30) (Table 4). The month wise variation of Na$^+$ and Cl$^-$ (Figure 8) for both fine and coarse mode aerosol show that during monsoon, coarse mode Na$^+$ and Cl$^-$ show higher concentrations whereas fine mode Na$^+$ and Cl$^-$ show minimum concentrations. This indicates that both the coarse mode Na$^+$ and Cl$^-$ have a common source *i.e.* sea salt particle, which could be transported by the southwest monsoon. Monsoon air masses reaching Darjeeling originate in the Bay of Bengal and incorporate a large amount of Na$^+$ and Cl$^-$. The inter-tropical convergence zone (ITCZ) is aligned at a rather northerly position during the monsoon season. The air masses are vertically raised by convective motion and transported horizontally by the upper air southerly monsoon flow to the Himalayas [12]. The higher concentrations of fine and coarse mode Cl$^-$ compared to Na$^+$ during the dry seasons (Jan–May, Oct–Dec) is believed to be associated with biomass and coal burning (domestic and railway). We also observed strong correlations between non-sea-K$^+$ and Cl$^-$ (R^2 = 0.82, n = 81) and between non-sea-SO$_4^{2-}$ and Cl$^-$ (R^2 = 0.78, n = 81) during dry seasons (Table 3) indicating the common biomass-burning source.

The average concentrations of K$^+$ in fine and coarse mode aerosol were 1.17±0.83 µg m^{-3} and 0.31±0.17 µg m^{-3}, respectively. Biomass burning could have the highest abundance of fine mode K$^+$ of all source emissions. The fine mode K$^+$ could be released in the atmosphere by the burning of vegetative scrap [28].

The average concentration of fine mode non-sea-K$^+$ during winter was much higher (2.12±0.4 µg m^{-3}) than premonsoon (1.37±0.8 µg m^{-3}), monsoon (1.15±0.7 µg m^{-3}) and post-monsoon (1.08±0.62 µg m^{-3}) which was due to the massive biomass burning around Darjeeling especially during night times in winter. Figure 9(A) shows the month wise variations of fine mode non-sea-K$^+$ which is similar to fine mode non-sea-SO$_4^{2-}$ variations. A strong correlation (R^2 = 0.78, n = 81) between non-sea-K$^+$ and non-sea-SO$_4^{2-}$ was also observed in fine mode aerosol during dry seasons (Table 3) indicating their common source of biomass burning.

The average concentrations of Ca^{2+} and Mg^{2+} in fine mode aerosol were 0.13±0.1 µg m^{-3} and 0.12±0.09 µg m^{-3} respectively and in coarse mode aerosol were 0.39±0.19 µg m^{-3} and 0.31±0.17 µg m^{-3} respectively. Figure 9(B) shows the monthly variations of non-sea-Ca^{2+} and non-sea-Mg^{2+} both in fine and coarse mode aerosol. Strong correlations were observed between non-sea-Ca^{2+} and non-sea-Mg^{2+} (Table 3) during dry seasons indicating their enrichment in aerosol mainly as dust aerosol. Non-sea-Ca^{2+} and non-sea-Mg^{2+} both show peaks during pre-monsoon both in fine and coarse mode aerosol. The higher concentrations of those mineral components during pre-monsoon could be related to the long-range transport of dust aerosol. The dust aerosols driven by the premonsoon westerlies are vertically advected to elevated altitudes (∼5 km) against the foothills of the Himalayas due to the enhanced convection and steep pressure gradient across the Himalayan-Gangetic region [29]. According to [29], the dust-rich aerosols from the Indo-Gangetic plain can "climb" the slope of the Himalayas in the premonsoon season. Similar concentrations of Ca^{2+} at two different altitudes, 800 and 3920 masl at two stations in Nepal Himalayan region during premonsoon was also observed showing the long-range transport from southwestern Asia and northern Africa [13]. Very high concentrations of coarse mode Ca^{2+} over a station near Thar deserts was also observed [30,31].
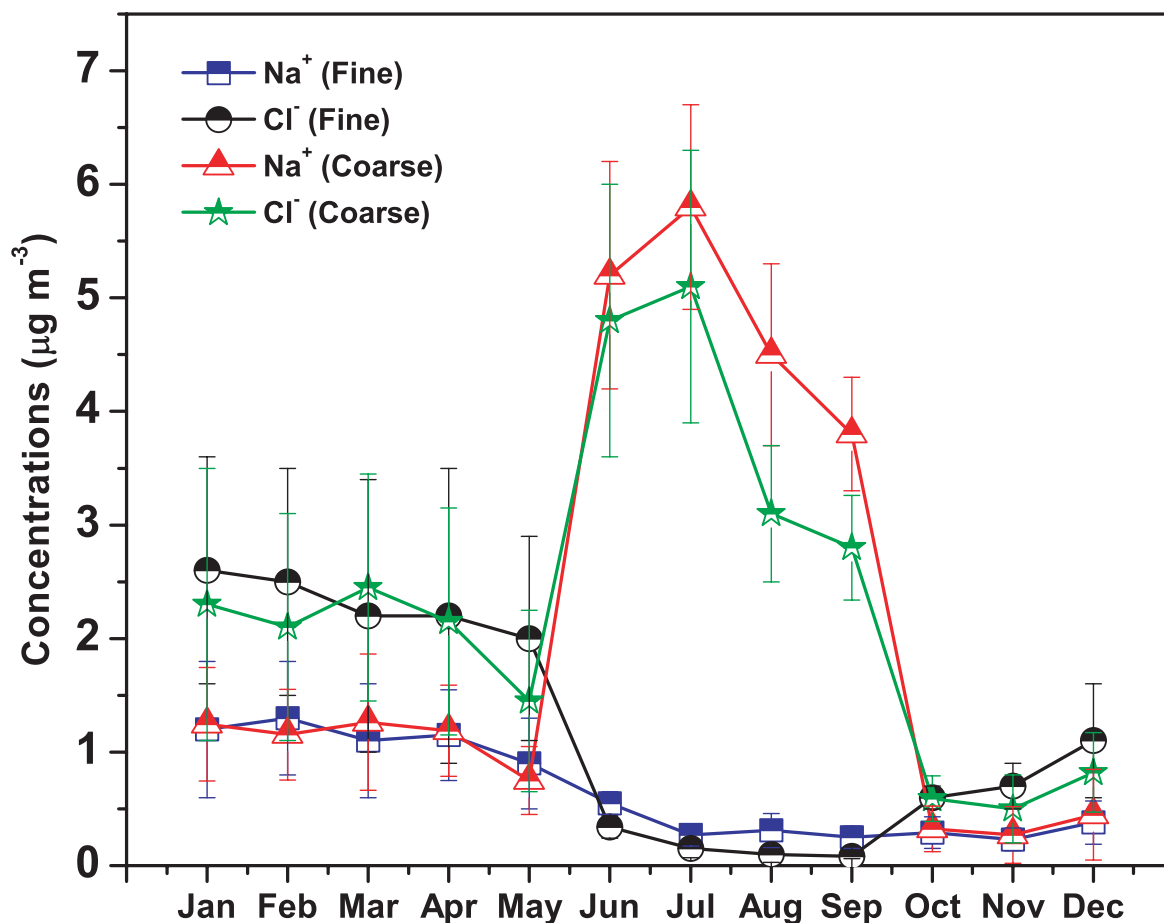
Figure 8. Seasonal variations of primary ionic species over Darjeeling.
doi:10.1371/journal.pone.0011122.g008

Using HYSPLIT_4 (Hybrid Single Particle Lagrangian Integrated Trajectory, www.arl.noaa.gov/ready/hysplit4.html) model developed by NOAA/ARL, back trajectories were computed for all sampling events at 0500 UTC. Two distinct source regions are identified, arid and semi-arid regions of western India including Thar deserts (45%) and upwind regions of Arabian deserts (32%), which are shown in figure 10A and 10B as representative figures. The percentage distributions of source regions (45% from Thar deserts and 32% from Arabian deserts) were determined based on the ratio of the number of events of the respective regions (using HYSPLIT) to the total number of sampling events. The loading of Ca^{2+} and Mg^{2+} over Darjeeling from Thar deserts was found to be higher than the Arabian deserts. The correlation of Ca^{2+} and Mg^{2+} with trace metals like Fe, Al, Si during premonsoon would be useful to put the evidence towards the transport of dust aerosol from distant regions. However the studies on the effect of dust aerosol on the total aerosol loading over Himalayan region and its effect on the optical properties of aerosol during premonsoon are under development.

The higher concentrations of Ca^{2+} over Ahmedabad (located near Thar desert in western India) compared to Darjeeling and other Himalayan regions (Table 1 and 2) indicate that the dust aerosol reach Himalayas after significant dilution. With the onset of rainy season (the Arabian Sea and Bay of Bengal branches of the southwest summer monsoon), the heavy dust loading significantly diminishes due to aerosol washout from the atmosphere. Non-sea-Ca^{2+} and non-sea-Mg^{2+} both show mini-

mum concentrations indicating the below cloud scavenging of dust aerosol due to heavy rain during monsoon (1783 mm). However, the negative concentration of coarse mode non-sea-Mg^{2+} during monsoon indicates that the entire coarse mode Mg^{2+} was from the marine source during monsoon.

2.4. Chloride depletion: interaction between marine and urban aerosol. Chloride depletion results when the acidic species, mainly nitrate, sulphate and some organic acids react with sea-salt particles and replace Cl^- in the form of HCl gas. NOx transforms into gaseous nitrous and nitric acid, which react with NaCl in sea-salt aerosol to form $NaNO_3$ and HCl. SO_2 oxidation and to a lesser extent H_2SO_4 vapor condensation on sea salt aerosols can also lead to chloride depletion. The reaction pathways are given as follows [32]:

$$NaCl(s,aq) + NO_3^-(s) \rightarrow NaNO_3(s) + Cl^-(g)$$
$$NaCl(s,aq) + SO_4^{2-}(s) \rightarrow Na_2SO_4(s) + Cl^-(g)$$
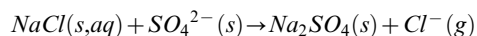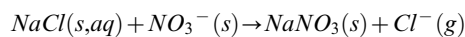
Those reactions given above occur especially when polluted urban aerosols and maritime aerosols are mixed with each other. Thus the extent of chloride depletion is an indication of the interaction between marine and urban aerosol as well as important in estimating the amount of nitrate and sulphate formed on sea-salt particles. Figure 11 shows the monthly variations of chloride depletion and it is clearly observed from the figure that only monsoon shows chloride depletion both in fine and coarse mode
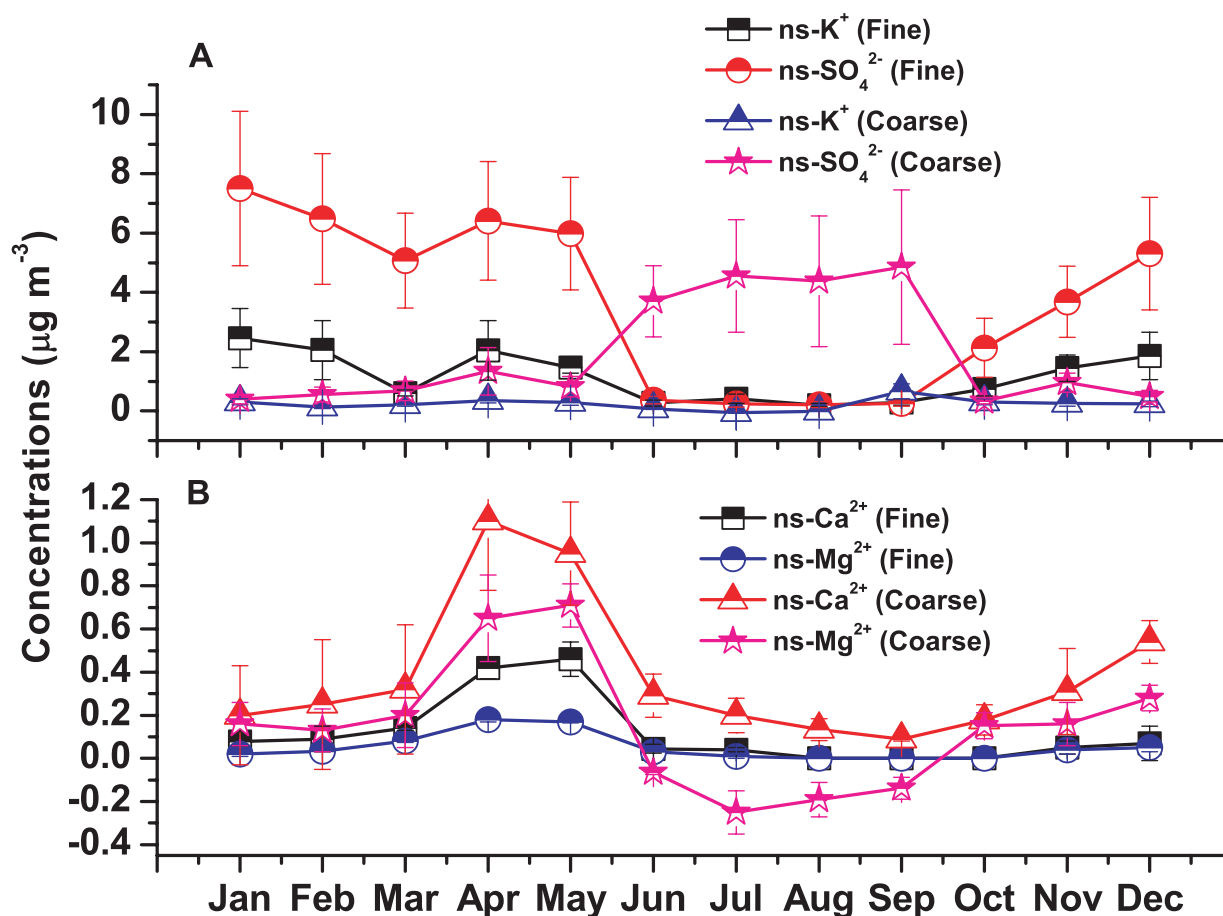
Figure 9. Seasonal variations of non-sea (ns) aerosol ionic species. A) Anthropogenic aerosols (biomass burning) and B) Natural aerosols (dust).
doi:10.1371/journal.pone.0011122.g009

aerosol. The percentage of Cl^- depletion (Cl^-_{dep}) can be calculated as follows [32]:

$$Cl^-_{dep}(\%) = \frac{\left([Cl^-]_{seawater,estimated} - [Cl^-]_{aerosol,measured}\right)}{[Cl^-]_{seawater,estimated}} \times 100$$

$$= \frac{\left(1.17[Na^+]_{aerosol,measured} - [Cl^-]_{aerosol,measured}\right)}{1.17[Na^+]_{aerosol,measured}} \times 100$$

Here, the source of measured Na^+ concentration in aerosol is assumed to be sea water only. In this study, the average depletion of Cl^- in fine mode aerosol ($61.2\pm13.3\%$) during monsoon was higher than coarse mode aerosol ($31.02\pm9.6\%$). It was suggested that the surface reaction mechanism is the principal explanation for higher depletion of smaller particles [33,34]. The dynamics of the chloride depletion reactions favor smaller particles because of their larger surface area distribution and longer atmospheric residence time. [32] observed that the Cl^- depletion decreases from 98% to 10% as particle size increases from 1.8 µm to 18 µm. [33] reported a reduction of chloride depletion of 90–100% at particle size of 1–2 µm to less than 40% at particle size of 8–15 µm for sea-salt particles in Finland.

An attempt was made to estimate the contribution of nitrate and non-sea-sulphate to the chloride depletion in fine and coarse mode aerosol. A ratio of the measured Na^+ concentrations in aerosol to the estimated original Cl^- concentration in sea salt was used to

determine the contribution of nitrate and non-sea-sulphate to chloride depletion. According to [33] the original chloride concentrations in sea salt can be determined as $[Cl^-]_{original} = [Cl^-]_{measured} + [NO_3^-]_{measured}$, assuming that chloride depletion results from nitrate formation process and the amount of measured nitrate is equal to the amount of lost chloride or $[Cl^-]_{original} = [Cl^-]_{measured} + [non-sea-SO_4^{2-}]_{measured}$, assuming that chloride depletion results from non-sea-sulphate formation process and the amount of measured non-sea-sulphate is equal to the amount of lost chloride or $[Cl^-]_{original} = [Cl^-]_{measured} + [NO_3^-]_{measured} + [non-sea-SO_4^{2-}]_{measured}$, assuming both nitrate and non-sea-sulphate are responsible for the depletion of chloride. Figure 12 shows the scatter plot of the ratios during monsoon for fine and coarse mode aerosol along with the ratio of measured $[Na^+]$ to measured $[Cl^-]$ in aerosol. The ratio, $[Na^+]/[Cl^-]$ in unreacted original sea water is 0.85.

Naturally the ratio, $[Na^+]/[Cl^-]$, in fine and coarse mode aerosol were higher than 0.85 because of chloride depletion. Interestingly, the ratios $[Na^+]/([Cl^-]+[NO_3^-])$ for coarse mode aerosol were found to be close to 0.85. This indicates that the measured coarse mode nitrate during monsoon was involved in chloride depletion. A strong correlation between coarse mode Na^+ and coarse mode NO_3^- during monsoon ($R^2 = 0.83$, n = 30) (Table 4) added further evidence to the above fact. On the other hand, the ratios $[Na^+]/([Cl^-]+[NO_3^-])$ for fine mode aerosol were quite lower than 0.85 indicating the overestimation of nitrate, *i.e.* the measured nitrate was not totally the nitrate from sea-salt but also from some other sources.
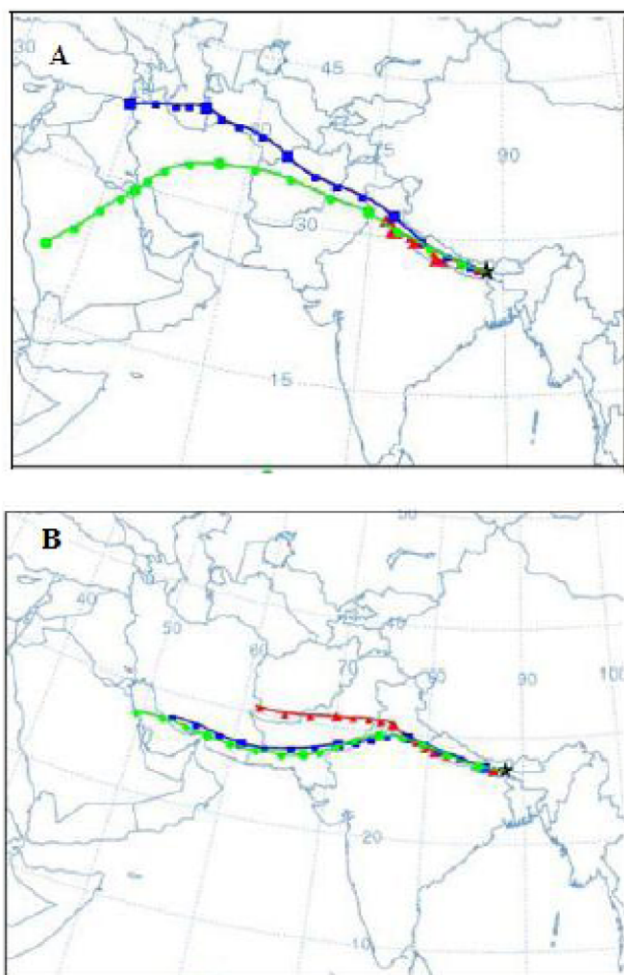
Figure 10. Long range transport of dust aerosol. A) From Thar deserts and B) From Arabian deserts.
doi:10.1371/journal.pone.0011122.g010

The ratios, $[Na^+]/([Cl^-]+[non\text{-}sea\text{-}SO_4^{2-}])$ in fine mode aerosol were close to 0.85. This indicates that the measured fine mode non-sea-sulphate during monsoon was totally involved in chloride depletion. We observed a strong correlation between Na^+ and fine mode non-sea-SO_4^{2-} ($R^2 = 0.78$, n = 30) (Table 4) during monsoon. Thus, we observed that non-sea-sulphate depleted chloride from fine mode sea salt aerosol whereas nitrate depleted chloride from coarse mode sea salt aerosol.

The chloride depletion from sea salt aerosol *i.e.* the interaction between marine (natural) and urban (anthropogenic) aerosol has major implications not only in changing the chemical composition of aerosol in different size modes but also it governs the rate of dry atmospheric removal of the species involved in chloride depletion. For example, here in this study the chloride depletion from coarse mode sea salt aerosol was found to govern the dry atmospheric removal of nitrate from the atmosphere. The dry depositional flux of nitrate in fine and coarse mode aerosol was calculated as follows:

$$\text{Dry depositional flux } (mg\,m^{-2}\,day^{-1}) =$$
$$\text{concentration}(mg\,m^{-3}) \times \text{deposition velocity}(m\,day^{-1})$$

Here, deposition velocity of nitrate in fine mode aerosol was considered to be $0.1\ cm\ s^{-1}$ and that in coarse mode was

considered to be $1\ cm\ s^{-1}$ [35]. It is relevant to state that these deposition velocities can be in error up to a factor of 3 [36]. The nitrate was found to be enriched mainly in fine mode aerosol as NH_4NO_3 during winter with the average deposition flux of $518 \pm 65\ mg\ m^{-2}\ day^{-1}$. On the other hand, coarse mode nitrate was found to be enriched as $NaNO_3$ after depleting chloride from sea salt aerosol during monsoon with a higher deposition flux of $1468 \pm 300\ mg\ m^{-2}\ day^{-1}$. Thus we observed that the interaction between natural marine aerosol and anthropogenic urban aerosol enhanced the rate of dry atmospheric removal of nitrate.

3. Acidity of aerosol: ionic balance and ionic ratios

Strong acidity in terms of nmol H^+ per m^3 of air is a parameter that characterizes the absolute acidity of atmospheric aerosols [37]. This is obtained from the total H^+ derived from the aqueous extract of atmospheric aerosols and is estimated using an ionic balance of the inorganic ionic species. On the other hand, free acidity (pH) characterizes the relative acidity of atmospheric aerosols and depends on the water content and composition of aerosol and relative humidity [36]. Here in this study we have given more emphasis on ionic balance in explaining the aerosol acidity. Although strong acidity is due to the strong acidic components in aerosols like nitrate and sulphate, we have estimated the acidity (total H^+ in nmol m^{-3}) using all the ionic species according to [38].

$$[H^+]_{total} = (2 \times [SO_4^{2-}] + [NO_3^-] + [Cl^-]) -$$
$$([Na^+] + [K^+] + [NH_4^+] + 2 \times [Ca^{2+}] + 2 \times [Mg^{2+}])$$

Figure 13 shows the month wise variations of $[H^+]_{total}$ and the equivalent ratio of the sum of cations to the sum of anions (Σ^+/Σ^-) in fine and coarse mode aerosol. It was observed that fine mode aerosol acidity ($[H^+]_{total}$) was much higher during dry seasons (73 nmol m^{-3}) compared to monsoon (-4.1 nmol m^{-3}) whereas coarse mode aerosol acidity was higher during monsoon (19 nmol m^{-3}) compared to dry seasons (-34.6 nmol m^{-3}). The ratio, Σ^+/Σ^-, ranged between 0.46 to 1.43 (Average: 0.84, Standard deviation: 0.29) in fine mode aerosol and between 0.9 to 1.95 (Average: 1.31, Standard deviation: 0.34) in coarse mode aerosol. The cation deficiency in fine mode aerosol could be attributed to H^+ whereas anion deficiency in coarse mode aerosol could be attributed to unanalyzed organic acid ions, carbonate, bicarbonate etc. The higher concentrations of nitrate, non-sea-sulphate and chloride during dry seasons increased $[H^+]_{total}$ in fine mode aerosol whereas the lower concentrations of non-sea-magnesium and non-sea-calcium along with higher concentration of nitrate during monsoon increased $[H^+]_{total}$ in coarse mode aerosol. Thus, the acidity of fine mode aerosol was mainly controlled by the species originated from fossil fuel and biomass burning whereas the acidity of coarse mode aerosol was mainly controlled by dust particles.

4. Sources of aerosol

4.1. Source apportionment by Principal Component Analysis. It is very important, and difficult as well, to identify the exact sources of the aerosol components in Darjeeling, the area under concern at the northeastern Himalayas, where composite anthropogenic activities including biomass burning and vehicular emission play a central role in loading of air pollutants in the atmosphere. Principal component analysis (PCA), a multivariate analysis technique [39] was used to identify possible sources of aerosols in Darjeeling. Each principal component (PC) shows correlation of each variable as loadings (loading greater than 0.5 was
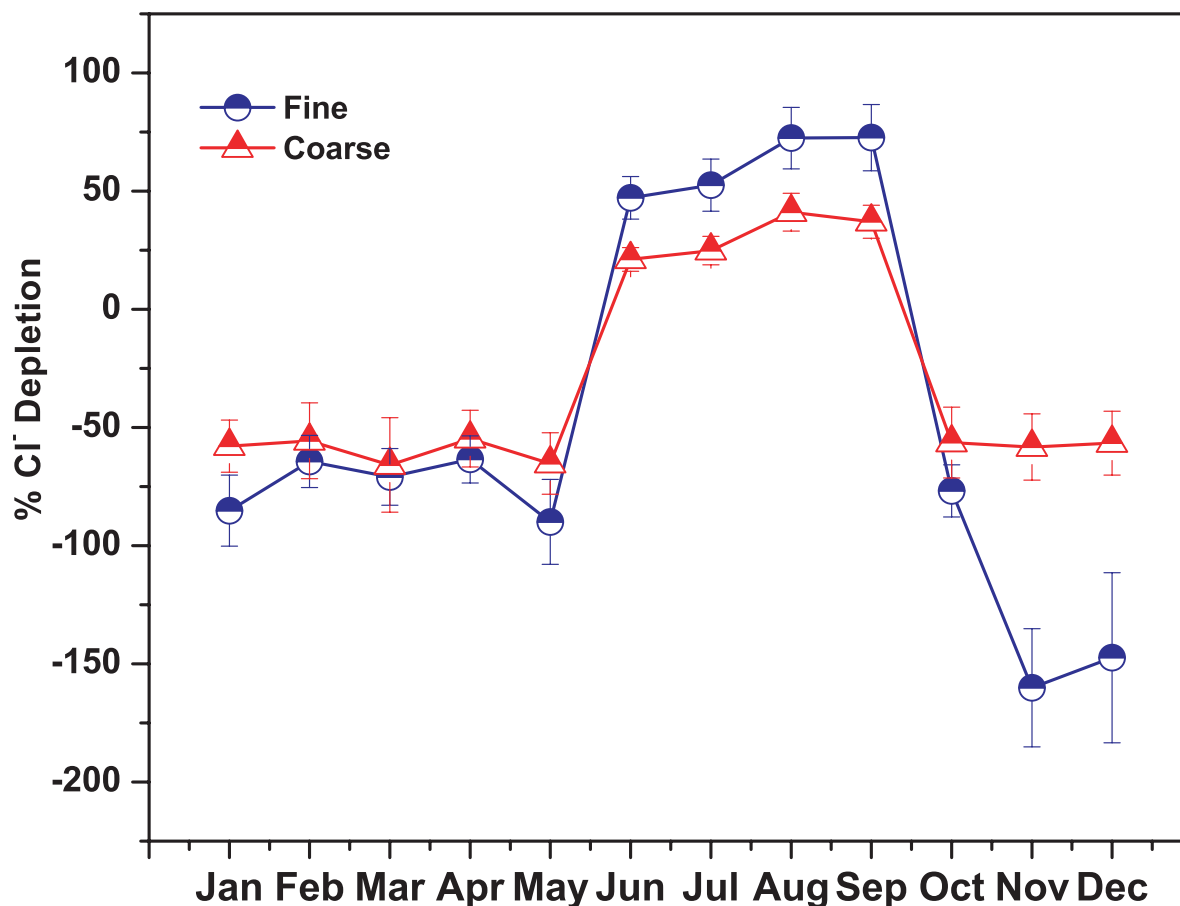
Figure 11. Seasonal variation of chloride depletion from sea-salt aerosol.
doi:10.1371/journal.pone.0011122.g011

considered to be statistically significant in this study). Since higher loading of particular variable in a PC can help in identifying the possible sources [40], the number of PCs selected (sources identified) should represent the sources that are relevant in the receptor domain. PCA was performed using the statistical software, SPSS (Statistical Package for the Social Sciences) [41] of version 16.0.2 using the data sets over the entire study period (n = 66).

For fine mode aerosol, three PCs were extracted (Figure 14). The first PC (PC1) shows the heavy loading of K^+, Cl^- and SO_4^{2-} with wind speed having 41.5% variance of the data set. These species in PC1 correspond to the massive biomass burning throughout the year mainly during winter in Darjeeling. The coal engine which is used for the Darjeeling Himalayan Railways is also a major source of these species in the atmosphere. Thus, PC1 indicates the loading of K^+, Cl^- and SO_4^{2-} as non-sea-K^+, non-sea-Cl^- and non-sea-SO_4^{2-} respectively. The negative loading of wind speed in this PC indicates the dispersion of these fine mode species favored by higher wind speed. The second PC (PC2) shows the heavy loading of NH_4^+, NO_3^-, SO_4^{2-} with 33.3% of the data variance. This PC is associated with the formation of secondary anthropogenic particles in the atmosphere. Different agricultural activities and usage of different ammoniated fertilizers in several tea gardens and also in tea processing plants, animal manure and human activities are the major sources for the emission of NH_3 and/or NH_4^+ in the atmosphere. The third PC (PC3) is moderately loaded with NH_4^+ and highly loaded with NO_3^- along with temperature with 16.4% of the data variance. This

indicates the emission of NOx from vehicular exhaust and its subsequent transformation to particulate nitrate mostly as ammonium nitrate. The negative loading of temperature in PC3 clearly indicates the inverse relation of formation of particulate nitrate with temperature as discussed earlier.

For coarse mode aerosol, four PCs were extracted (Figure 14). The first PC (PC1) is highly loaded with the Na^+, Cl^- and Mg^{2+} having 40.5% data variance. This indicates the loading of sea salt aerosol. The second PC (PC2) shows the heavy loading of Ca^{2+}, Mg^{2+} along with wind speed with the moderate loading of K^+. This explains 34.2% of the data variance and indicates the enrichment of calcium, magnesium and a fraction of potassium as non-sea-calcium, non-sea-magnesium and non-sea-potassium from soil dust particles. The loading of wind speed in this PC indicates the resuspension of soil dust in the atmosphere favored by the higher wind speed. The third PC (PC3) shows the loading of Na^+ and NO_3^- with the data variance of 14.6%. This indicates the interaction of sea salt aerosol (NaCl) with nitrate (particulate or gaseous) and the production of coarse mode nitrate through the chloride displacement reactions discussed earlier. The fourth PC (PC4) shows the higher loading and association of SO_4^{2-} only with 6.4% of data variance. The loading of sulphate singly in PC4 indicates the enrichment of non-sea-sulphate in coarse mode which is due to the aqueous phase transformation of SO_2 to sulphate in high relative humidity during monsoon. The higher concentration of non-sea-sulphate during monsoon in coarse mode aerosol has already been discussed.
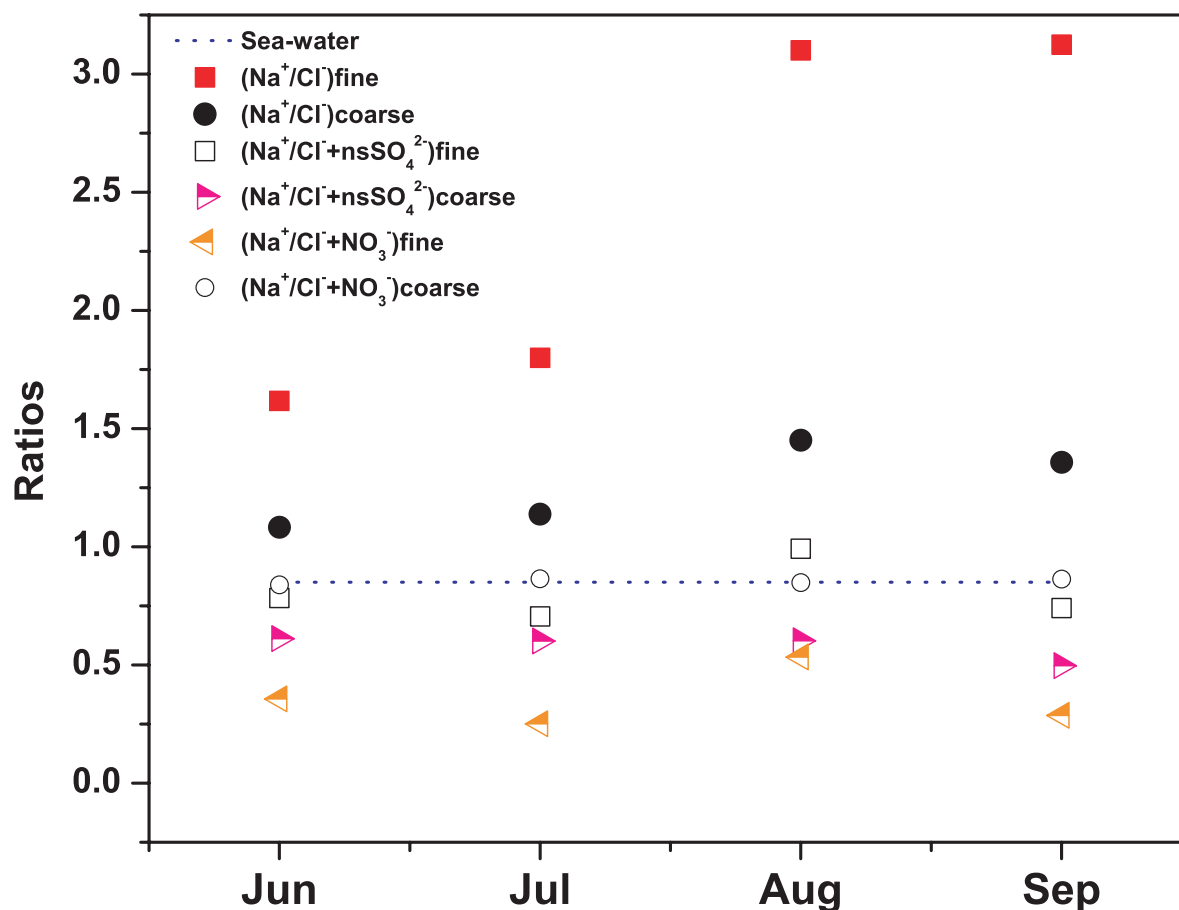
Figure 12. Modified ratios of sodium to chloride indicating contribution of nitrate and non-sea (ns) sulphate to chloride depletion.
doi:10.1371/journal.pone.0011122.g012

4.2. Source identification by air mass parcels using HYSPLIT back trajectory. In order to find out the possibility of atmospheric transport of different species from outside of Darjeeling, backward trajectories for air parcels arriving at the sampling site during the sampling period were calculated with the HYSPLIT_4 model. Back trajectories were computed for all sampling events at 0500 UTC. The Final Run (FNL) meteorological data was used for the trajectory calculation.

Different air masses travel through different regions and bring different chemical components with the aerosol, thus the distribution of chemical components among different air masses could shed some light on their possible sources. Based on the transport pathways of air masses, three typical air mass trajectories, representing local, continental (other than local), and marine were found in Darjeeling and have been shown in Figure 14. Marine air parcels are mainly from the South East (Bay of Bengal) and South West (Arabian Sea) and could bring a large amount of marine aerosol. Continental air masses are mainly from North West and could bring several crustal species from inland emissions. Table 5 presents the distributions of mass concentrations of major ionic species along with $[H^+]_{total}$ (nmol m^{-3}) and Σ^+/Σ^- ratio both in fine and coarse mode aerosol for three types of air masses.

The higher contribution of local and continental sources to the fine mode aerosol was observed with a little influence of marine sources while the concentration of coarse mode aerosol was found to be higher from the marine source regions than the local and

other continental sources. The concentrations of Na$^+$ and Cl$^-$ follow the same sequence and their coarse mode concentrations were found to be the highest for marine air parcel, indicating the strong influence from the sea. The higher concentrations of fine mode Cl$^-$ for continental and local sources indicate the influence of biomass and coal burning. The higher concentrations of coarse mode Ca^{2+} and Mg^{2+} from local and continental sectors indicate the resuspension of local and wind blown soil dust particles. The concentration of coarse mode Mg^{2+} from marine sectors shows the influence of sea salt Mg^{2+}. Local and continental sectors show the higher concentrations of fine and coarse mode K$^+$ indicating the strong influence of biomass burning and soil dust aerosol respectively. The higher concentrations of fine mode NH$_4^+$, NO$_3^-$ and SO$_4^{2-}$ from local and continental sectors show a very strong influence of anthropogenic activities whereas coarse mode NO$_3^-$ shows higher concentration from marine sectors. This coarse mode nitrate from marine sectors is not sea salt nitrate rather it indicates the interaction between sea salt aerosol and gas phase HNO$_3$ and its association with sodium through chloride displacement reaction discussed earlier. Fine mode aerosol shows higher $[H^+]_{total}$ and lower Σ^+/Σ^- (104.8 nmol m^{-3} and 0.59, respectively) from the local compared to continental (39.2 nmol m^{-3} and 0.79, respectively) and marine (−11.3 nmol m^{-3} and 1.2, respectively) source regions whereas coarse mode aerosol shows maximum $[H^+]_{total}$ and minimum Σ^+/Σ^- ratio (8.03 nmol m^{-3} and 0.96, respectively) from marine source compared to local (−57.5 nmol m^{-3} and 1.51, respectively) and continental sources
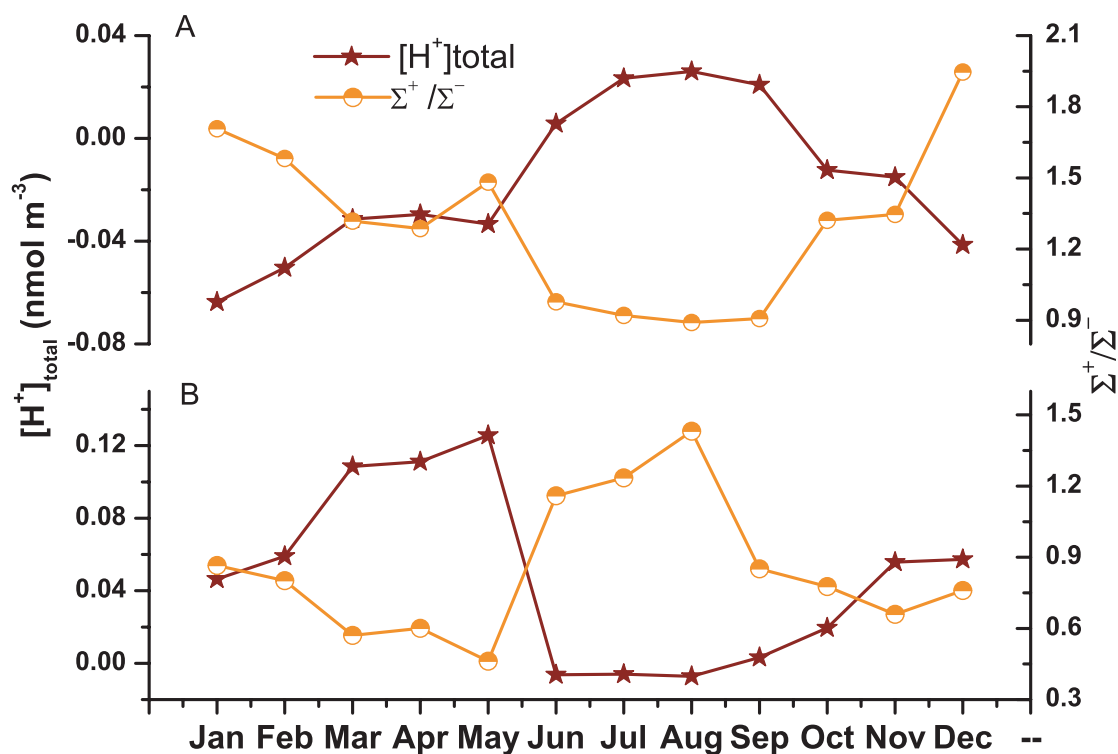
Figure 13. Seasonal variation of acidity of aerosol and ionic ratios.
doi:10.1371/journal.pone.0011122.g013

(-2.6 nmol m^{-3} and 1.03, respectively). Thus, local and continental fine mode aerosols were more acidic than coarse mode aerosol whereas marine fine mode aerosols were less acidic compared to coarse mode aerosol.

Based on the Principal Component Analysis (for source types) and HYSPLIT trajectory model (for source regions) the percentage distribution of several source types of water soluble ions from different source regions (local, continental and marine) in fine and coarse mode aerosol were determined and depicted in Figure 15. In this figure, the percentage distribution of source regions was determined based on the ratio of the number of events of the respective regions (using HYSPLIT) to the total number of events. The figure also describes the percentage distribution of ionic species between primary and secondary species. The percentage of the primary species was determined based on the ratio of sum of the concentrations of chloride, sodium, potassium, calcium and magnesium to the total ionic concentration of aerosol whereas ammonium, nitrate and sulphate were used for the determination of percentage of secondary species in a similar way. Principal component analysis was done using data set from each sector (local, continental and marine) separately for fine and coarse mode aerosol. That means the percentage distribution of various source types (shown in Figure 15) is actually the percentage of variation obtained from factor analysis by PCA.

Figure 15 shows that, 80% of the ionic species originated from the local and other continental sources and 20% was from the marine source. Biomass burning and vehicular emissions (non-sea-potassium, non-sea-sulphate, non-sea-chloride, nitrate) were the major sources for fine mode local and continental aerosols whereas dust particles (non-sea-calcium and magnesium) were the major source for coarse mode local and continental aerosols. On the other hand, the major source for fine and coarse mode marine aerosol was sea salt aerosols enriched mainly with sodium and chloride.

Conclusions

The major findings of this study can be summarized as:

(1) The average concentration of fine mode aerosol is found to be higher than coarse mode aerosol during dry seasons whereas monsoon shows higher loading of coarse mode aerosol compared to fine mode.

(2) This study discusses the formation pathways of major secondary aerosol components. Nitrate is found to exist as ammonium nitrate in fine mode aerosol during winter whereas during monsoon nitrate exists as sodium nitrate in coarse mode aerosol. Photochemical oxidation of SO_2 is the major pathway for the formation of sulphate during premonsoon whereas some other aqueous phase transformation processes are important pathways during winter in sulphate formation.

(3) There is a major contribution of non-sea-sulphate and nitrate in the chloride depletion from fine and coarse mode sea salt aerosols, respectively. The chloride depletion, *i.e.* the interaction between marine and urban aerosol, is found to govern the dry removal of nitrate from the atmosphere. The nitrate which is found to be enriched mostly in fine mode during dry seasons gets enriched in coarse mode during monsoon because of the chloride displacement from coarse mode sea salt aerosol. Thus nitrate is found to be deposited (dry or free fall deposition) at a faster rate during monsoon compared to dry seasons.

(4) The acidity of fine mode aerosol is found to be higher in dry seasons compared to monsoon whereas the acidity of coarse mode acidity is found to be higher in monsoon compared to dry seasons. Non-sea-sulphate and nitrate are found to govern the acidity of fine mode aerosol whereas non-sea-calcium and non-sea-magnesium govern the coarse mode acidity.
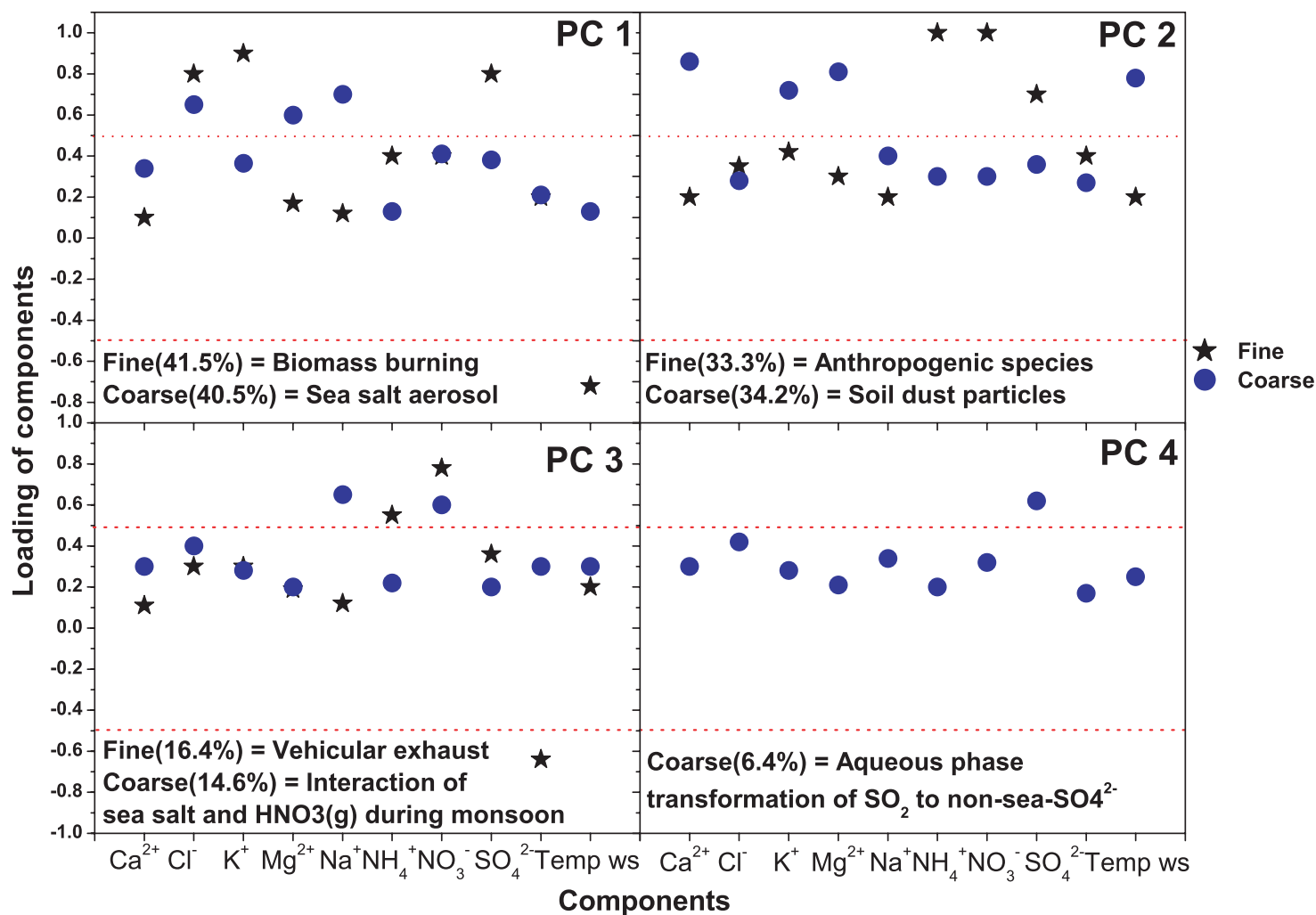
Figure 14. Aerosol source apportionment by Principal Component Analysis.
doi:10.1371/journal.pone.0011122.g014

(5) Three major source regions like local, continental (mainly from north-western part of India) and marine (Bay of Bengal and Arabian Sea) sources are identified based on HYSPLIT backward trajectory model. Local and other continental source regions contribute 80% with high loading of secondary anthropogenic species whereas the contribution from marine source regions is 20% enriched with primary sea salt particles.

(6) Biomass burning and vehicular emissions are the major sources for fine mode local and continental aerosols with higher acidity whereas soil dust particles are the major source for coarse mode local and continental aerosols with lower acidity. On the other hand, the major source for fine and coarse mode marine aerosol is sea salt aerosols with higher acidity in coarse mode.

Table 5. Concentrations of water soluble ionic species in fine and coarse mode aerosols from different source regions.

|		Aerosol ($\mu g\ m^{-3}$)	Na^+ ($\mu g\ m^{-3}$)	NH_4^+ ($\mu g\ m^{-3}$)	K^+ ($\mu g\ m^{-3}$)	Ca^{2+} ($\mu g\ m^{-3}$)	Mg^{2+} ($\mu g\ m^{-3}$)	Cl^- ($\mu g\ m^{-3}$)	NO_3^- ($\mu g\ m^{-3}$)	SO_4^{2-} ($\mu g\ m^{-3}$)	$[H^+]_{total}$ (nmol m^{-3})	$\sum^+/\sum^-$
Local	Fine	34.1	0.4	1.3	1.7	0.10	0.13	2.4	5.1	5.8	104.8	0.59
	Coarse	18.2	1.9	0.08	0.6	0.61	0.45	1.6	1.6	2.1	−57.5	1.51
Continental	Fine	44.2	0.9	1.1	1.1	0.26	0.16	1.2	4.1	4.5	39.2	0.79
	Coarse	12.2	0.7	0.05	0.22	0.40	0.35	1.3	1.1	1.8	−2.6	1.03
Marine	Fine	9.2	0.7	0.2	0.7	0.03	0.07	0.7	0.8	2.1	−11.3	1.20
	Coarse	26.4	3.9	0.03	0.1	0.2	0.12	3.3	2.1	1.6	8.03	0.96

doi:10.1371/journal.pone.0011122.t005
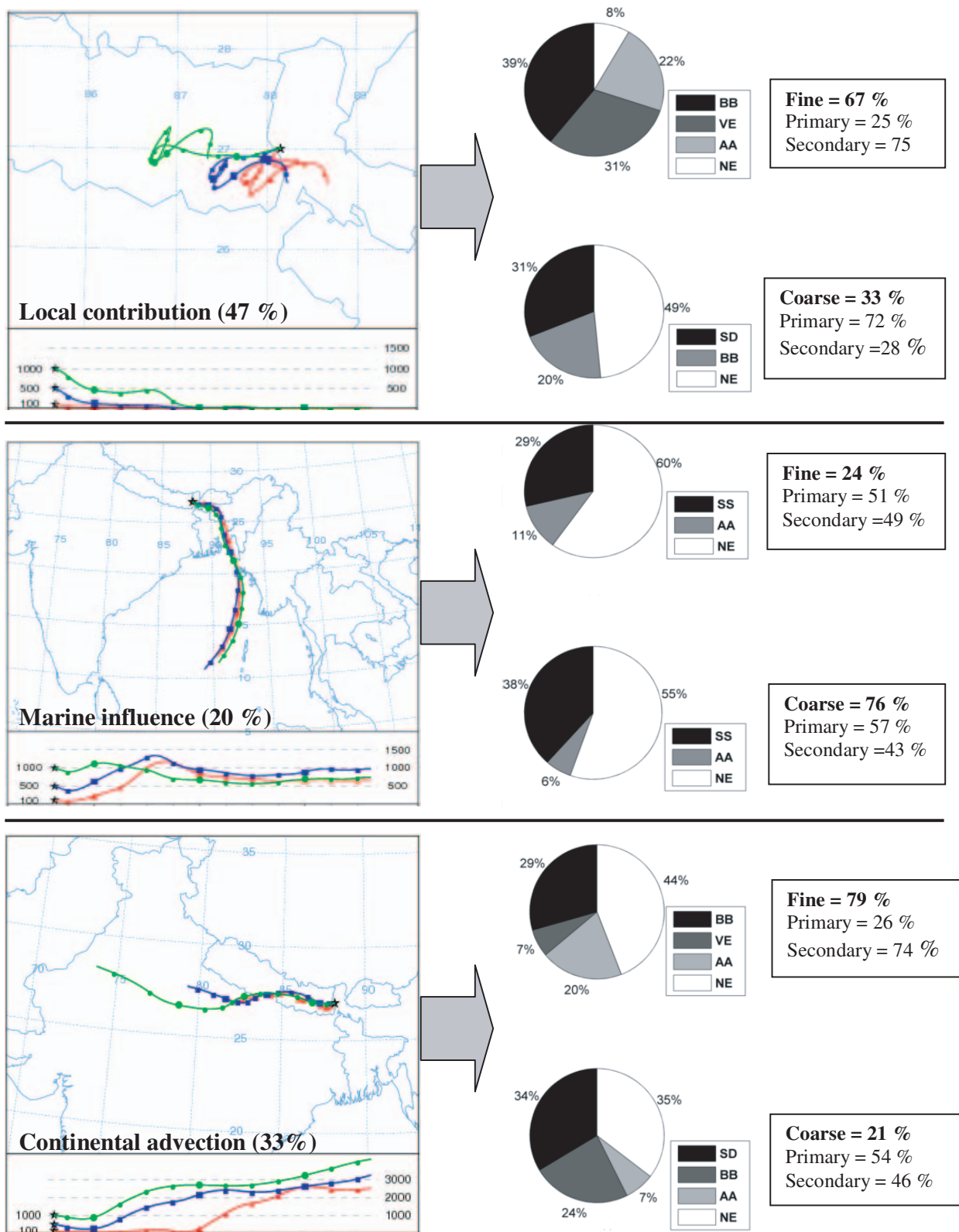
Figure 15. Several source types of aerosol from different source regions. Contributions from local and continental sources (with higher enrichment of fine aerosols) were found to be higher comparative to marine sources (with higher enrichment of coarse aerosols).
doi:10.1371/journal.pone.0011122.g015

Acknowledgments

Author Contributions

Conceived and designed the experiments: AC SR. Performed the experiments: AC AA AKS. Analyzed the data: AC MKS SKG. Contributed reagents/materials/analysis tools: ST PCSD. Wrote the paper: AC SKG SR.

References

1. IPCC (2007) Intergovernmental Panel on Climate Change. Fourth Assessment Report. Cambridge University Press, Cambridge, Section 2.2. 37 p.

2. Gautam R, Hsu NC, Lau KM, Tsay SC, Kafatos M (2009) Enhanced pre-monsoon warming over the Himalayan-Gangetic region from 1979 to 2007. Geophys Res Lett 36: L07704. doi: 10.1029/2009GL037641.

3. Ramanathan V, Li F, Ramana MV, Siva PS, Kim D, et al. (2007) Atmospheric Brown Clouds: Hemispherical and regional variations in long range transport, absorption and radiative forcing. J Geophys. Res 112: D24S91. doi:10.1029/2006JD008124.

4. Gautam R, Liu Z, Singh RP, Hsu NC (2009) Two contrasting dust-dominant periods over India observed from MODIS and CALIPSO. Geophys Res Lett 36: L06813. doi: 10.1029/2008GL036967.

5. Mayewski PA, Jeschke PA (1979) Himalayan and Trans-Himalayan glacier fluctuations since AD 1812. Arct Alp Res 11: 267–287.

6. Ashish A, Joshi V, Sharma A, Anthwal S (2006) Retreat of Himalayan glaciers indicator of climate change. Nature and Science 4: 53–60.

7. Decesari S, Facchini MC, Carbone CL, Giulianelli M, Rinaldi E, et al. (2009) Chemical composition of PM10 and PM1 at the high-altitude Himalayan station Nepal Climate Observatory-Pyramid (NCO-P) (5079 m a.s.l.). Atmos Chem Phys Discuss 9: 25487–25522.

8. Safai PD, Momin GA, Rao PSP, Pillai AG, Tiwari S, et al. (1995) Chemical nature of the aerosols at a rural site in India. IASTA Bulletin. S1–S5.

9. Momin GA, Rao PSP, Safai PD, Ali K, Naik MS, et al. (1999) Atmospheric aerosol characteristic Studies at Pune and Thiruvananthapuram during INDOEX programme-1998. Curr Sci 76: 985–989.

10. Wake CP, Dibb JE, Mayewski PA, Zhongqin L, Zichu X (1994) The chemical composition of aerosols over the Eastern Himalayas and Tibetan Plateau during low dust periods. Atmos Environ 28: 695–704.

11. Shrestha AB, Wake CP, Dibb JE (1997) Chemical composition of aerosol and snow in the High Himalayas during the summer monsoon season. Atmos Environ 31: 2815–2826.

12. Shrestha AB, Cameron PW, Dibb JE, Mayewski PA, Whitlow SI, et al. (2000) Seasonal variations in aerosol concentrations and compositions in the Nepal Himalayas. Atmos Environ 34: 3349–3363.

13. Carrico CM, Bergin HM, Shrestha AB, Dibb JE, Gomes L, et al. (2003) The importance of carbon and mineral dust to seasonal aerosol properties in the Nepal Himalayas. Atmos Environ 37: 2811–2824.

14. Gajananda K, Kuniyal JC, Momin GA, Rao PSP, Safai PD, et al. (2005) Trend of atmospheric aerosols over the north western Himalayan region, India. Atmos Environ 39: 4817–4825.

15. Chatterjee A, Dutta C, Sen S, Ghosh K, Biswas N, et al. (2006) Formation, transformation, and removal of aerosol over a tropical mangrove forest. J Geophys Res 111: D24302. doi: 10.1029/2006JD007144.

16. Kaupp H, McLachlan MS (1999) Atmospheric particle size distributions of polychlorinated dibenzo-p-dioxins and dibenzofurans (PCDD/Fs) and polycyclic aromatic hydrocarbons (PAHs) and their implications for wet and dry deposition. Atmos Environ 33: 85–95.

17. Giuliacci M (1988) Physical and dynamical climatology of the Po Valley, Regional Meteo. Service, Bologna (in Italian).

18. Lau KM, Kim MK, Kim KM (2006a) Asian monsoon anomalies induced by aerosol direct effects. Clim Dyn 26: 855–864.

19. Rastogi N, Sarin MM (2005) Long-term characterization of ionic species in aerosols from urban and high-altitude sites in western India: Role of mineral dust and anthropogenic sources. Atmos Environ 39: 5541–5554.

20. Mozurkewich M (1993) The dissociation constant of ammonium nitrate and its dependence on temperature, relative humidity and particle size. Atmos Environ 27: 261–270.

21. Wang Y, Zhuang G, Zhang X, Huang K, Xu C, et al. (2005) The ion chemistry, seasonal cycle, and sources of PM2.5 and TSP aerosol in Shanghai. Atmos Environ 39: 3771–3784.

22. Kim HS, Huh JB, Hopke PK, Holsen TM, Yi SM (2007) Characteristics of the major chemical constituents of $PM_{2.5}$ and smog events in Seoul, Korea in 2003 and 2004. Atmos Environ 41: 6762–6770.

23. Dasgupta PK, Campbell SW, Al-Horr RS, Rahmat Ullah SM, Li J, et al. (2007) Conversion of sea salt aerosol to NaNO3 and the production of HCl: Analysis of temporal behavior of aerosol chloride/nitrate and gaseous HCl/HNO3 concentrations with AIM. Atmos Environ 41: 4242–4257.

24. Ohta S, Okita T (1990) A chemical characterization of atmospheric aerosol in Sapporo. Atmos Environ 24A: 815–822.

25. Seinfeld JH (1986) Atmospheric Chemistry and Physics of Air Pollution. Wiley, New York. 348 p.

26. Xiu G, Zhang D, Chen J, Huang X, Chen Z, et al. (2004) Characterization of major water-soluble inorganic ions in size-fractionated particulate matters in Shanghai campus ambient air. Atmos Environ 38: 227–236.

27. Kulshrestha MJ, Kulshrestha UC, Parashar DC, Vairamani M (2003) Estimation of SO_4^{2-} contribution by dry deposition of SO_2 onto the dust particles in India. Atmos Environ 37: 3057–3063.

28. Zelenka MP, Wilson WE, Chow JC, Lioy PJ (1994) A combined TTFA/CMB receptor modeling approach and its application to air pollution sources in China. Atmos Environ 28: 1425–1435.

29. Gautam R, Hsu NC, Lau KM, Tsay SC, Kafatos M (2009) Enhanced pre-monsoon warming over the Himalayan-Gangetic region from 1979 to 2007. Geophys Res Lett 36: L07704. doi:10.1029/2009GL037641.

30. Rastogi N, Sarin MM (2009) Quantitative chemical composition and characteristics of aerosols over western India: One-year record of temporal variability. Atmos Environ 43: 3481–3488.

31. Kumar A, Sudheer AK (2008) Mineral and anthropogenic aerosols in Arabian Sea-atmospheric boundary layer: Sources and spatial variability. Atmos Environ 42: 5169–5182.

32. Zhuang H, Chan CK, Fang M, Wexler AS (1999) Size distributions of particulate sulphate, nitrate and ammonium at a coastal site in Hong Kong. Atmos Environ 33: 843–853.

33. Pakkanen TA (1996) Study of formation of coarse particle nitrate aerosol. Atmos Environ 30: 2475–2482.

34. McInnes LM, Covert DS, Quinn PK, Germani MS (1994) Measurements of chloride depletion and sulfur enrichment in individual sea-salt particles collected from the remote marine boundary layer. J Geophys Res 99: 8257–8268.

35. Rastogi N, Sarin MM (2007) Chemistry of Precipitation Events and Inter-Relationship with Ambient Aerosols over a Semi-Arid Region in Western India. J Atmos Chem 56: 149–163.

36. Duce RA, Liss PS, Merril JT, Atlas EL, Buat-Menard P, et al. (1991) The atmospheric input of trace species to the world ocean. Global Biogeochem Cycles 5: 193–259.

37. Pathak RK, Peter KK, Chan LCK (2004) Characteristics of aerosol acidity in Hong Kong. Atmos Environ 38: 2965–2974.

38. Lippmann M, Xiong JQ, Li W (2000) Development of a continuous monitoring system for PM10 and components of PM2.5. Appl Occup Environ Hyg 15: 57–67.

39. Storch Von, Zwiers FW (1999) Statistical analysis in climate research. Cambridge University Press. 298 p.

40. Maenhaut W, Cafmeyer J (1987) Particle induced X-ray emission analysis and multivariate techniques: an application to the study of the sources of respirable atmospheric particles in Gent, Belgium. J Trace Microprobe Tech 5: 135–158.

41. SPSS (2003) Advanced Statistics Manual. SPSS/PC+V 3.0. SPSS Inc., 444 North Michigan Avenue, Chicago IL 60611.

42. Rengarajan R, Sarin MM, Sudheer AK (2007) Carbonaceous and inorganic species in atmospheric aerosols during wintertime over urban and high-altitude sites in North India. J Geophys Res 112: D21307. doi: 10.1029/2006JD008150.

43. Venkataraman C, Reddy CK, Josson S, Reddy MS (2002) Aerosol size and chemical characteristics at Mumbai, India, during the INDOEX-IFP (1999). Atmos Environ 36: 1979–1991.

44. Kulshrestha UC, Saxena A, Kumar N, Kumari KM, Srivastava SS (1998) Chemical composition and association of size differentiated aerosols at a suburban site in a semi-arid tract of India. J Atmos Chem 29: 109–118.